

1 **Composition and sources of carbonaceous aerosol in the European Arctic at Zeppelin**
2 **Observatory, Svalbard (2017 to 2020)**

3
4 Karl Espen Yttri^{1*}, Are Bäcklund¹, Franz Conen², Sabine Eckhardt¹, Nikolaos Evangeliou¹, Markus
5 Fiebig¹, Anne Kasper-Giebl³, Avram Gold⁴, Hans Gundersen¹, Cathrine Lund Myhre¹, Stephen Matthew
6 Platt¹, David Simpson^{5,6}, Jason D. Surratt^{4,7}, Sönke Szidat⁸, Martin Rauber⁸, Kjetil Tørseth¹, Martin
7 Album Ytre-Eide¹, Zhenfa Zhang⁴ and Wenche Aas¹

8
9 ¹The Climate and Environmental Research Institute NILU, Kjeller, Norway.

10 ²Department of Environmental Sciences, University of Basel, Basel, Switzerland

11 ³TU Wien, Institute of Chemical Technologies and Analytics, 1060 Vienna, Austria

12 ⁴Department of Environmental Sciences and Engineering, Gillings School of Global Public Health,
13 University of North Carolina at Chapel Hill, Chapel Hill, NC 27599, USA

14 ⁵EMEP MSC-W, Norwegian Meteorological Institute, Oslo, Norway

15 ⁶Department of Earth & Space Sciences, Chalmers Univ. Technology, Gothenburg, Sweden

16 ⁷Department of Chemistry, College of Arts and Sciences, University of North Carolina at Chapel Hill,
17 Chapel Hill, NC 27599, USA

18 ⁸Department of Chemistry, Biochemistry and Pharmaceutical Sciences & Oeschger Centre for Climate
19 Change Research, University of Bern, 3012 Bern, Switzerland

20
21 *To whom correspondence should be addressed: E-mail address: key@nilu.no

42 **Abstract**

43 We analyzed long-term measurements of organic carbon, elemental carbon, and source-specific organic
44 tracers from 2017 to 2020 to constrain carbonaceous aerosol sources in the rapidly changing Arctic.
45 Additionally, we used absorption photometer (Aethalometer) measurements to constrain equivalent
46 black carbon (eBC) from biomass burning and fossil fuel combustion, using Positive Matrix
47 Factorization (PMF).

48 Our analysis shows that organic tracers are essential in understanding Arctic carbonaceous
49 aerosol sources. Throughout 2017 to 2020, levoglucosan exhibited bimodal seasonality, reflecting
50 emissions from residential wood combustion (RWC) in the heating season (November to May) and from
51 wildfires (WF) in the non-heating season (June to October), demonstrating a pronounced inter-annual
52 variability in the influence of WF. Biogenic secondary organic aerosol (BSOA) species (2-methyltetrols)
53 from isoprene oxidation was only present in the non-heating season, peaking in July to August. Warm
54 air masses from Siberia led to a substantial increase in 2-methyltetrols in 2019 and 2020 compared to
55 2017 to 2018. This highlights the need to investigate the contribution of local sources vs. long-range
56 atmospheric transport (LRT), considering the temperature sensitivity of biogenic volatile organic
57 compounds emissions from Arctic vegetation. Tracers of primary biological aerosol particles (PBAP),
58 including various sugars and sugar-alcohols, showed elevated levels in the non-heating season, albeit
59 with different seasonal trends, whereas cellulose had no apparent seasonality. Most PBAP tracers and
60 2-methyltetrols peaked during influence of WF emissions, highlighting the importance of measuring a
61 range of source specific tracers to understand sources and dynamics of carbonaceous aerosol. The
62 seasonality of carbonaceous aerosol was strongly influenced by LRT episodes, as background levels are
63 extremely low. In the non-heating season, the organic aerosol peak was as influenced by LRT as was
64 elemental carbon during the Arctic Haze period.

65 Source apportionment of carbonaceous aerosol by Latin Hypercube Sampling showed mixed
66 contributions from RWC (46%), fossil fuel (FF) sources (27%), and BSOA (25%) in the heating season.
67 In contrast, the non-heating season was dominated by BSOA (56%), with lower contributions from WF
68 (26%) and fossil fuel sources (15%).

69 Source apportionment of eBC by PMF showed that fossil fuel combustion dominated eBC ($70 \pm$
70 2.7%), whereas RWC ($22 \pm 2.7\%$) was more abundant than WF ($8.0 \pm 2.9\%$). Modeled BC
71 concentrations from FLEXPART attributed an almost equal share to fossil fuel sources ($51 \pm 3.1\%$) and
72 to biomass burning. Both FLEXPART and the PMF analysis concluded that RWC is a more important
73 source of (e)BC than WF. However, with a modeled RWC contribution of $30 \pm 4.1\%$ and WF of $19 \pm$
74 2.8% , FLEXPART suggests relatively higher contributions to eBC from these sources. Notably, the BB
75 fraction of EC was twice as high as that of eBC, reflecting methodological differences between source
76 apportionment by LHS and PMF. However, important conclusions drawn are unaffected, as both
77 methods indicate the presence of RWC- and WF-sourced BC at Zeppelin, with a higher relative BB
78 contribution during the non-heating season.

79 In summary, organic aerosol ($281 \pm 106 \text{ ng m}^{-3}$) constitute a significant fraction of Arctic PM_{10} ,
80 although surpassed by sea salt aerosol ($682 \pm 46.9 \text{ ng m}^{-3}$), mineral dust ($613 \pm 368 \text{ ng m}^{-3}$) and typically
81 non-sea-salt sulfate SO_4^{2-} ($314 \pm 62.6 \text{ ng m}^{-3}$), originating mainly from anthropogenic sources in winter
82 and from natural sources in summer.

83

84 **1 Introduction**

85 The arctic is warming significantly faster than the rest of the planet due to Arctic amplification (Serreze
86 and Barry, 2011; Schmale et al., 2021). These rapid changes affect atmospheric transport and removal
87 of Arctic aerosols (Jiao and Flanner, 2016), aerosol relative source contributions (Heslin-Rees et al.,
88 2020), vegetation and the carbon cycle (Kramshoj et al., 2016).

89 Long-range atmospheric transport (LRT) of air masses from lower latitudes is an important
90 driver of the Arctic aerosol burden since local emissions are relatively much lower (e.g., Quinn et al.,
91 2007). However, the importance of LRT may be decreasing since low latitude anthropogenic aerosol
92 emissions are declining (Coen et al., 2020), while high latitude sources are increasing in importance.
93 These include, for example, increased wildfires (WF) (McCarty et al., 2021), sea salt aerosol (SSA)
94 (Heslin-Rees et al., 2020), aeolian mineral dust (MD) following glacial retreat (Zwaafink et al., 2016),
95 primary biological aerosol particles (PBAP) due to thawing permafrost and Arctic greening (Myers-
96 Smith et al., 2020), which is also likely increasing biogenic volatile organic compounds emission rates
97 and hence biogenic secondary organic aerosol (BSOA) (Hallquist et al., 2009). These changes in sources
98 may also change Arctic aerosol physical-chemical properties and hence their climate impact. Some
99 PBAP are efficient ice nucleating particles at high temperatures (Tobo et al., 2019), while BSOA might
100 act as cloud condensation nuclei or influence their activity (Riipinen et al., 2011), and have negative
101 feedback to the Arctic climate (Paasonen et al., 2013). Given its relevance for the Arctic climate, there
102 is a marked interest in exploring the concentration, activation temperature, composition, sources, origin,
103 and seasonality of Arctic ice nucleating particles and cloud condensation nuclei, as shown by Creamean
104 et al. (2018; 2019; 2020; 2022), Hartmann et al. (2019; 2020), and Freitas et al. (2023). The aerosol
105 indirect effect is particularly important in the Arctic, as mixed phase clouds have a long lifetime,
106 possibly due to a lack of ice nucleating particles (Solomon et al., 2018), thus changes ice nucleating
107 particles are deemed more important than cloud condensation nuclei regarding Arctic cloud radiative
108 properties (Solomon et al., 2018).

109 Understanding changes in local aerosol emissions and formation, shifts in aerosol LRT, and thus
110 alterations in aerosol chemical composition, are essential for understanding their climate impact and the
111 evolving Arctic environment. Long-term observations are crucial to such an understanding. This is
112 especially true for carbonaceous aerosol (CA), though the situation is somewhat more favourable for
113 black carbon (BC), as it has been a focus of attention due to its significant impact on climate and albedo
114 (Clarke and Noone, 1985; Pueschel and Kinne, 1995; Hansen and Nazarenko, 2004; Eleftheriadis et al.,
115 2009; Hirdmann et al., 2010). A second exception is methane sulfonic acid (MSA) with time series from

116 1977 at Alert (Sharma et al., 2019) and 1980 at Barrow (Quinn et al., 2009), though its role in aerosol
117 formation, growth, and radiative forcing is still a matter of ongoing research (Hodshire et al., 2019).

118 Significant contributions to Organic matter (OM) of Eurasian origin to Arctic Haze (AH) have
119 been suggested since the 1970s (Quinn et al., 2007), quantified mostly as a residual fraction (Quinn et
120 al., 2002) or from measurements of selected organic species (Li et al., 1993). Even short-term, direct,
121 measurements of organic carbon (OC) or OM are scarce (e.g., Hansen et al., 2014; Barrett et al., 2015;
122 Ferrero et al., 2019), limiting our understanding of even basic parameters such as seasonality, annual
123 mean, or inter annual variability. The nearly two-year long study of Ricard et al. (2002) at Sevetjärvi
124 (Finland) is one of three exceptions, though at a latitude of $< 70^\circ$ N, and hence not representative of the
125 high Arctic, with e.g., lower AH and more biogenic volatile organic compounds in summer. Barret et
126 al. (2017) report 1 year of OC data at Barrow, whereas Moschos et al. (2022) presented the most
127 comprehensive study on Arctic OA to this date with up to 3 years of data from 8 Arctic sites.

128 OC levels are not useful in elucidating sources per se, and supporting information is generally
129 needed. For example, elemental carbon (EC) (or equivalent black carbon, eBC) demonstrates the
130 presence of OC from fossil fuel (FF) combustion and biomass burning (BB), essential to source
131 apportionment efforts and monitoring of the otherwise unperturbed Arctic atmosphere. Winiger et al.
132 (2019), attributed $25 \pm 16\%$ of EC to BB in winter and $42 \pm 19\%$ in summer by radiocarbon (^{14}C)
133 analysis in their Pan-Arctic study. Further separation of BB into residential wood combustion (RWC),
134 WF and agricultural waste burning requires inclusion of satellite observations such as MODIS
135 (Moderate Resolution Imaging Spectroradiometer) (Giglio et al., 2003), and transport modelling (Stohl
136 et al., 2006), although seasonality can be a useful qualifier. Stohl et al. (2013) pointed to gas and oil
137 industry flaring as a major source, contributing 42% to Arctic annual mean BC surface concentrations.
138 ^{14}C analysis by Barrett et al. (2017) shows that contemporary OC from biogenic emissions dominated
139 in summer, while contemporary and fossil OC levels were approximately equally large in winter.
140 Moschos et al. (2022) used positive matrix factorization (PMF) on spectral data derived from water-
141 soluble organic carbon extracts, analyzed off-line using an aerosol mass spectrometer. Their study
142 identified three factors dominated by anthropogenic sources (Oxygenated Organic Aerosol, Arctic Haze,
143 and Primary Organic Aerosol) and three factors associated with natural emissions (Methane Sulfonic
144 Acid-Related Organic Aerosol, Primary Biological Organic Aerosol, and Biogenic Secondary Organic
145 Aerosol). These factors exhibited distinct seasonal patterns, with the first three dominating in winter and
146 the latter three in summer.

147 Source specific organic tracers identified in the Arctic include levoglucosan, mannosan and
148 galactosan (e.g., Schneidemesser et al., 2009; Fu et al., 2013; Zangrando et al., 2013; Hu et al., 2013a;
149 Yttri et al., 2014; Feltracco et al., 2020), which are combustion products of cellulose and hemi-cellulose
150 serving to trace biomass burning emissions (Simoneit et al., 1999). Sugars, sugar-alcohols (here:
151 glucose, fructose, trehalose, arabitol, and mannitol) and cellulose are used for tracing PBAP (Graham et
152 al., 2003; Elbert et al., 2007; Sanchez-Ochoa et al., 2007), with sugar-alcohols typically associated with

153 yeast and fungal spores, and sugars linked to pollen, fern spores and other giant bioaerosol (Graham et
154 al., 2003). Cellulose, a primary component of plant cell walls, is used to trace plant debris (Sanchez-
155 Ochoa et al., 2007). Sugars and sugar-alcohols have previously been detected in Arctic aerosol (e.g., Fu
156 et al., 2009b; Fu et al., 2013; Feltracco et al., 2020), but cellulose has not been reported in these studies.
157 Oxidation products of isoprene (e.g., 2-methyltetrols), monoterpenes (e.g., 3-Methyl-1,2,3-butane-
158 tricarboxylic acid), and sesquiterpenes (e.g., β -caryophyllinic acid) are all BSOA species previously
159 detected in the Arctic aerosol (Fu et al., 2009a; Fu et al., 2013; Hansen et al., 2014; Hu et al., 2013).
160 Most studies measuring organic tracers in the Arctic have been limited to short time periods or specific
161 seasons, lacking a comprehensive understanding of the seasonal, annual and interannual variability of
162 sources and their impact on Arctic CA. Notable exceptions are the one-year study of Hansen et al. (2014)
163 and Yttri et al. (2014), along with the multi-seasonal investigation of Feltracco et al. (2020).

164 Lack of long-term OA measurements limits knowledge of Arctic aerosol mass closure. Further,
165 OA speciation, needed for source attribution and for studying its impact on cloud condensation nuclei
166 and ice nucleating particles is scarce. Here, we present four years of OC and EC, organic tracer, and
167 eBC_{BB} and eBC_{FF} measurements made at the high Arctic Zeppelin Observatory (Ny-Ålesund, Svalbard),
168 providing multiyear insights to Arctic CA and the fundamental knowledge needed to understand changes
169 in Arctic cloud condensation nuclei and ice nucleating particles and hence the impact of a changing
170 Arctic on regional and global climate.

171

172 **2 Experimental**

173 **2.1 Sampling site**

174 The Zeppelin Observatory (78°5' N 11°5' E, 472 m above sea level, asl) is located on the Zeppelin
175 Mountain on the 20 km long and 10 km wide Brøgger peninsula, 2 km south of the remote Ny-Ålesund
176 settlement on the west coast of the Spitsbergen Island in the Svalbard archipelago (Norway, Fig. 1; Platt
177 et al., 2022). The 26 km long Kongsfjorden to the northeast and the 88 km long Forland straight in the
178 west, surround the peninsula. The Observatory lies in the northern Arctic tundra zone, surrounded by
179 barren ground largely consisting of bare stones, and occasionally a thin layer of topsoil with scarce
180 ground vegetation, mostly growing on plains at lower altitudes, and snowpacks, and glaciers. There is
181 very little influence of emissions from the Ny-Ålesund settlement, as the Observatory is typically above
182 the boundary layer.

183 The Svalbard climate reflects its high Northern latitude, but is moderated by the North Atlantic
184 Current, with substantially higher temperatures than at corresponding latitudes in continental Russia and
185 Canada, particularly in winter. Hence, the Kongsfjorden basin is considered relatively verdant due to its
186 favorable micro-climate, and ~180 plant species, 380 mosses, and 600 lichens are registered on the
187 Svalbard Archipelago (Vegetation in Svalbard, 2023). However, a short growing season (June to
188 August), 4 months of polar night, and 8 to 9 months of snow (Fig. 2) do not provide optimal conditions
189 for growth (Karlsen et al., 2014). Annual precipitation in Western Svalbard is around 400 mm.

190 The Zeppelin Observatory is part of many networks including the European Evaluation and
191 Monitoring Program (EMEP, www.emep.int), the Global Atmospheric Watch (GAW,
192 <https://public.wmo.int/en/programmes>), the Arctic Monitoring and Assessment Program (AMAP,
193 www.amap.no), and is included in the EU infrastructure ACTRIS (Aerosols, Clouds and Trace gases
194 Research InfraStructure Network, www.actris.eu)

195 196 **2.2 Sampling, handling, and storage of ambient aerosol filter samples**

197 We used a Digitel high-volume sampler (PM₁₀ inlet, flow rate 666 L min⁻¹, filter face velocity 72.1 cm
198 s⁻¹) to obtain ambient aerosol filter samples. We placed the sampling inlet 2 m above the Observatory
199 roof and 7 m above ground level. We collected aerosol particles on pre-fired (850 °C; 3 h) quartz fiber
200 filters (PALLFLEX Tissuequartz 2500QAT-UP; 150 mm in diameter) at a weekly time resolution. There
201 was some variability in sampling time, typically due to harsh weather conditions. We used a quartz fiber
202 filter behind quartz fiber filter (QBQ) set up to estimate the positive sampling artifact of OC (McDow
203 and Huntzicker, 1990). We shipped the filters in their respective filter holders, wrapped in baked
204 aluminum foil, and placed them in double zip lock bags. Before exposure and analysis, we stored the
205 samples in a freezer (-18°C). For each 1.5 month of sampling, we assigned one field blank, which was
206 treated in the same manner regarding preparation, handling, transport, and storage as the exposed filters,
207 except that they were not inserted in the sampler.

208 We collected the aerosol filter samples from 5 January 2017 to 4 January 2021 as part of the
209 Norwegian national monitoring programme (Aas et al., 2020)

210 211 **2.3 Measurement of OC and EC**

212 We performed Thermal-optical analysis (TOA) using the Sunset Lab OC/EC Aerosol Analyzer. We
213 used transmission for charring correction and operated the instrument according to the EUSAAR-2
214 temperature program (Cavalli et al., 2010). As part of the joint EMEP/ACTRIS quality assurance and
215 quality control effort, we regularly intercompared the performance of the OC/EC instrument (e.g.,
216 Cavalli et al., 2016).

217 218 **2.4 Measurement of organic tracers**

219 **2.4.1 Monosaccharide anhydrides, 2-methyltetrols, sugars, and sugar-alcohols**

220 We determined concentrations of monosaccharide anhydrides, sugar-alcohols, 2-methyltetrols,
221 monomeric and dimeric sugars in PM₁₀ filter samples using ultra-performance liquid chromatography
222 (UPLC) (Vanquish UPLC, Thermo) in combination with Orbitrap Q-Exactive Plus (Thermo Fischer
223 Scientific) operated in the negative electrospray ionization (ESI) mode: resolution 70 000 FWHM (full
224 width at half maximum) at 200 Dalton.

225 We added isotopically labelled internal standard to filter punches (2 × 1.5 cm²), which were
226 submerged in precleaned tetrahydrofuran (THF) (2 mL) in separate screw neck amber glass vials, which

227 we subjected to ultrasonic extraction (30 min). We transferred the solute to a centrifuge tube using
228 pipetting and repeated this step twice. Afterward, we evaporated the solute to 0.4 mL, spun it (10 min;
229 2000 rpm), transferred and evaporated it to dryness in a screw neck amber glass vial. The sample volume
230 was redissolved in 0.25 mL precleaned THF/Milli-Q water (55:45) and whirlmixed before analysis. The
231 extraction procedure was equal to Dye and Yttri (2005). We used two columns in series for separation
232 (two 3.0 mm × 150 mm HSS T3, 1.8 μm, Waters Inc.), using isocratic elution (Milli-Q; 18.2 MΩ),
233 flushing with acetonitrile (High purity) at the end of the run. The Milli-Q water was purified using and
234 EDS-Pak Polisher, containing activated coal (Merck, Darmstadt, Germany), and a LC-Pak cartridge
235 (Merck, Darmstadt, Germany) containing reversed-phase silica.

236 We identified all species based on retention time and mass spectra of authentic standards, using
237 isotope-labelled standards of levoglucosan, galactosan, mannitol, arabitol, trehalose and glucose as
238 recovery standards (Table S1 in Yttri et al., 2021). The limit of detection (LOD) was 1 to 3 pg m⁻³ for
239 the monosaccharide anhydrides, 1 pg m⁻³ for the 2-methyltetrols, 4 pg m⁻³ for the sugar-alcohols, 6 pg
240 m⁻³ for the dimeric sugars and 8 pg m⁻³ for the monomeric sugars.

241

242 **2.4.2 Measurement of cellulose**

243 We based the analysis of free cellulose on the saccharification of cellulose and subsequently quantified
244 the glucose produced, following the method by Kunit and Puxbaum (1996). We switched the final
245 detection of glucose from a photometric method to HPAEC PAD (high-performance anion-exchange
246 chromatography with pulsed amperometric detection), similar to Qi et al., 2020). We extracted filter
247 aliquots with a citrate buffer (0.05 M citric acid) adjusted to pH 4 and added Thymol to a final
248 concentration of 0.05% to prevent bacterial growth. We enhanced extraction by ultrasonic agitation. We
249 added enzymes (Trichoderma reesei cellulase; Aspergillus Niger cellobiase), which had been precleaned
250 by ultrafiltration to reduce glucose blanks, for saccharification. We stopped saccharification (at 45 °C)
251 after 24 h by heating the samples to 80 °C. We analyzed glucose on a Dionex ICS 3000 equipped with
252 a CarboPac MA1 column, using a sodium hydroxide gradient reaching from 480 mM NaOH to 630 mM.
253 We corrected results with the free glucose contained in the samples.

254

255 **2.5 Radiocarbon measurements**

256 We conducted ¹⁴C-measurements of TC and EC by complete combustion of the untreated quartz fiber
257 filter and after removal of OC, respectively, using thermal-optical analysis (760 °C, pure O₂) coupled
258 with on-line measurement in an accelerator mass spectrometer (Agrios et al., 2015). For a detailed
259 description of the analytical method and data processing, see Rauber et al. (2023).

260

261 **2.5.1 Selection criteria for samples subject to radiocarbon analysis**

262 We picked 1 – 2 filter samples for each month of the year from samples collected from 2017 to 2018 to
263 capture the seasonal variability in source composition (Table S3). No valid solution was found for the

264 sample 05 – 13.12.2017, using the Latin Hypercube Sampling (LHS) approach (Sect. 2.8), hence the
265 low coverage for December (6%) compared to September (77%). We pooled two consecutive samples
266 for the months of June, July, August, September, October, and December to meet the LOD (3 µg C) for
267 EC. Moreover, we aimed for the front/back filter carbon content ratio >3, but this criterion was not met
268 for one of the samples in June, September, October, and for two samples in December.

269 We analyzed ¹⁴C-TC on both front and back filters, while ¹⁴C-EC was analyzed only on front
270 filters. To measure ¹⁴C-EC, we used three circular punches (22 mm diameter) from the filter sample
271 aliquot (16.6 cm²). We used the remaining front filter area (5.2 cm²) for ¹⁴C-TC analysis, along with an
272 equivalent area of the back filter.

273

274 **2.6 Measurement of the aerosol absorption coefficient by multi wavelength Aethalometer**

275 We obtained measurements of aerosol absorption coefficient (Babs) using a 7-wavelength (370, 470,
276 520, 590, 660, 880, and 950 nm) absorption photometer (AE33 Aethalometer, Magee Scientific)
277 downstream of a PM₁₀ inlet, yielding equivalent black carbon (eBC) by normalization with co-located
278 EC measurements. We determined two eBC categories using a novel application of positive matrix
279 factorization (PMF) (Yttri et al., 2021; Platt et al., in prep.). These categories were based on the Aerosol
280 Ångström Exponent (AAE), with one having a low AAE (~1), resulting from efficient combustion of
281 mainly liquid fossil fuel, denoted eBC_{FF}, and the other having a high AAE (~1.6), mainly associated
282 with biomass burning (eBC_{BB}) and possibly residential coal combustion.

283

284 **2.7 Auxiliary data**

285 We downloaded concentrations of SO₄²⁻, Cl⁻, Na⁺, K⁺, Mg²⁺, Ca²⁺, Al, Fe, Mn, and Ti from the EBAS
286 data repository (<https://ebas-data.nilu.no>). Inorganic anions and cations were obtained using a NILU
287 stacked filter unit (SFU) collecting aerosol particles on Teflon filters (2 µm pore, 47 mm Zefluor Teflon,
288 Gelman Sciences). The SFU has a downward-facing inlet that effectively reduces the sampling
289 efficiency for aerosol particles with an equivalent aerodynamic diameter (EAD) larger than 10 µm
290 (Zwaafink et al., 2022). Elements were obtained from paper filters (Whatman 41) using a high-volume
291 air sampler with an inlet discriminating against aerosol particles with an EAD larger than 3 µm.

292 We calculated sea salt (ss) aerosol (SSA) according to equations 1 – 5, and mineral dust (MD)
293 according to equations 6 and 7. We assumed Al, Fe, Mn, and Ti to be associated exclusively with mineral
294 dust and present as Al₂O₃, Fe₂O₃, MnO, and TiO₂ (Alastuey et al., 2016). Si data was not available and
295 thus estimated based on an empirical factor (eq. 7), assumed present as SiO₂.

296

$$297 \text{ [SSA]} = \text{[Na}^+] + \text{[Cl}^-] + \text{[ssK}^+] + \text{[ssMg}^{2+}] + \text{[ssCa}^{2+}] + \text{[ssSO}_4^{2-}] \quad (\text{eq. 1})$$

298

$$299 \text{ [ssK}^+] = \text{[Na}^+] \times 0.037 \quad (\text{eq. 2})$$

$$300 \text{ [ssMg}^{2+}] = \text{[Na}^+] \times 0.12 \quad (\text{eq. 3})$$

301 $[\text{ssCa}^{2+}] = [\text{Na}^+] \times 0.038$ (eq. 4)

302 $[\text{ssSO}_4^{2-}] = [\text{Na}^+] \times 0.252$ (eq. 5)

303

304 $[\text{MD}] = [\text{SiO}_2] + [\text{Al}_2\text{O}_3] + [\text{Fe}_2\text{O}_3] + [\text{MnO}] + [\text{TiO}_2]$ (eq. 6)

305

306 $[\text{SiO}_2] = 2.5 \times [\text{Al}_2\text{O}_3]$ (eq. 7)

307

308 **2.8 Source apportionment of carbonaceous aerosol by Latin Hypercube Sampling**

309 We used a Latin Hypercube Sampling (LHS) approach (Gelenscer et al., 2007; Yttri et al., 2011a) for
310 source apportionment of CA, using ^{14}C , organic tracers, and OC and EC measurements from 13 samples
311 (Table S3) as input. We quantified seven CA fractions: EC from combustion of biomass (EC_{bb}) and
312 fossil fuel (EC_{ff}), OC from combustion of biomass (OC_{bb}) and from fossil fuel sources (OC_{ff}), primary
313 biological aerosol particles (OC_{PBAP}), being the sum of plant debris (OC_{pbc}) and fungal spores (OC_{pbs}),
314 and secondary organic aerosol (SOA) from biogenic precursors (OC_{BSOA}). Our calculations were based
315 on similar equations and emission ratios (ER) to those presented in Yttri et al. (2011a), except that we
316 used ^{14}C -EC to calculate OC_{BB} and EC_{BB} . We have provided updated equations and ERs in Tables S1 to
317 S2. At a remote site like Zeppelin where BB emissions originate from distant source regions, ^{14}C -EC
318 seems a better option for apportioning BB emission than levoglucosan, assuming significant depletion
319 of levoglucosan under such conditions. Calculated concentrations and fractions of the CA categories are
320 presented in Tables S3 and S4. The NH-season was covered by 98 days, while the heating (H) season
321 was covered by 54 days.

322

323 **2.9 FLEXPART modelling**

324 We calculated BC concentrations at Zeppelin using the Lagrangian particle dispersion model
325 FLEXPART version 10.4 (Pisso et al., 2019). FLEXPART released computational particles every 3 h
326 for the whole study period at the Zeppelin Observatory, which were tracked backward in time. The
327 model was driven by ERA5 (Hersbach et al., 2020) assimilated meteorological analyses from the
328 European Centre for Medium-Range Weather Forecasts (ECMWF) with 137 vertical layers, a horizontal
329 resolution of $0.5^\circ \times 0.5^\circ$, and one-hour temporal resolution. We kept the particles in the simulation for
330 30 days after release, sufficient to include most BC emissions arriving at the site, given a typical BC
331 lifetime of 1 week (Bond et al., 2013). FLEXPART simulates dry and wet deposition of gases or aerosols
332 (Grythe et al., 2017), turbulence (Cassiani et al., 2014), unresolved mesoscale motions (Stohl et al.,
333 2005), and includes a deep convection scheme (Forster et al., 2007). Footprint emission sensitivities
334 were calculated at spatial resolution of $0.5^\circ \times 0.5^\circ$. We assumed that BC has a density of 1500 kg m^{-3} ,
335 following a logarithmic size distribution with an aerodynamic mean diameter of $0.25 \mu\text{m}$ and a
336 logarithmic standard deviation of 0.3 (Long et al., 2013).

337 The footprint emission sensitivities express the probability of any release occurring in each grid-

338 cell to reach the receptor site. When coupled with gridded emissions from any emission inventory, it
339 can be converted to modelled concentration at the receptor site. To derive the contribution to receptor
340 BC from different sources, we combined each gridded emission sector (e.g., gas flaring, transportation)
341 with the footprint emission sensitivity. We used anthropogenic emissions from the latest version (v6b)
342 of the ECLIPSE (Evaluating the CLimate and Air Quality ImPacts of ShortlivEd Pollutants) dataset,
343 which is an upgraded version of the previous version 5a, as described by Klimont et al. (2017). The
344 inventory (provided with a spatial resolution of $0.5^\circ \times 0.5^\circ$, monthly) includes:

- 345
- 346 • Industrial combustion (IND) – emissions from industrial boilers and industrial production processes
- 347 • Energy production (ENE) – combustion processes in power plants and generators.
- 348 • Residential and commercial sector (DOM) – combustion in heating, cooking stoves, and boilers in
- 349 households, public, and commercial buildings.
- 350 • Waste treatment and disposal sector (WST) – emissions from waste incineration and treatment.
- 351 • Transport sector (TRA) – emissions from all land-based transport of goods, animals, and persons
- 352 on road and off-road networks, including domestic shipping and aviation.
- 353 • Emissions from international shipping activities (SHP).
- 354 • Gas flaring (FLR) – emissions from oil and gas facilities.
- 355

356 The ECLIPSEv6b dataset provides emission data at 5-years intervals. These emissions are then
357 interpolated to annual emissions according to the trend in geographical areas considered in ECLIPSE
358 (Klimont et al., 2017). The temporal variation in the emissions of all sectors was provided by IIASA
359 (Klimont et al., 2017). WF emissions were adopted from the Global Fire Emission Dataset version 4.1
360 (GFEDv4.1). The product combines satellite information on fire activity and vegetation productivity to
361 estimate gridded monthly burned area and fire emissions, as well as scalars that we can use to calculate
362 higher temporal resolution emissions. All data are publicly available for use in large-scale atmospheric
363 and biogeochemical modelling (van der Werf et al., 2017). Emission factors to compute BC emissions
364 are based on Akagi et al., (2011). The spatial resolution of the current version (v4) is of $0.25^\circ \times 0.25^\circ$,
365 daily.

366 To distinguish between modelled BC_{bb} and BC_{ff} , we combined contributions to receptor
367 concentrations from (i) DOM and WF, and (ii) ENE, FLR, IND, WST, SHP and TRA, respectively.

368

369 **3 Results and discussion**

370 Monthly mean concentrations of OC, EC, and organic tracers at Zeppelin Observatory are presented in
371 Fig. 2 and Fig. 3, and annual and seasonal means in Table 1. Our study is the first presenting eBC_{BB} and
372 eBC_{FF} data (Fig. 2) derived from multiwavelength aethalometer measurements in the Arctic, and we
373 compare them with BC_{BB} and BC_{FF} data obtained from the FLEXPART model (Table 3; Fig. 4; Fig S1)

374 and with EC_{BB} and EC_{FF} data from the LHS-approach (Sect. 3.2.1) (Table 4; Table S3 to S4). CA source
375 apportionment by the LHS-approach is presented in Fig. 5 and Tables S3 to S4. We discuss our data
376 according to the periods June to October, representing the growing season and the non-heating season
377 (NH-season), and November to May covering the non-growing season and the heating season (H-
378 season). These are obviously not absolute definitions. Phenomena of high relevance to the Arctic
379 aerosol, such as Boreal WF emissions thus largely reside in the NH-season, whereas accumulation of
380 anthropogenic emissions from Eurasia in winter and spring, known as AH, is part of the H-season.
381 Comparison is made with Birkenes Observatory (Southern Norway), representative of the lowest CA
382 levels in regional background Europe (Yttri et al., 2021) (Table S5 and S6), with Ispra, a regional
383 background site in the Po Valley (Northern Italy), one of Europe's most polluted regions (Table 5S),
384 and the Trollhaugen Observatory (Antarctica) (S7).

385

386 **3.1 Elemental carbon and organic carbon**

387 The interannual variabilities of EC (34%) and OC (38%) were comparable to SO_4^{2-} (40%). Like OC,
388 SO_4^{2-} can have both primary or secondary sources, originate from LRT or local emissions, and stem
389 from natural as well as anthropogenic sources. Notably, its time series spans back to 1991 (Platt et al.,
390 2022). The annual mean concentrations ranged from 6.5 to 16.3 ng Carbon (C) m^{-3} for EC and from 90.3
391 to 197 ng C m^{-3} for OC. These levels are amongst the lowest globally, still notably higher compared to
392 Antarctica (1.9 ng EC m^{-3} ; 12.2 ng OC m^{-3}) (Table S7) (Rauber et al., in prep.). Particulate OC (OC_P)
393 had an estimated conservative concentration of 68.3 to 165 ng C m^{-3} after accounting for the positive
394 sampling artifact (OC_B). CA levels were particularly high in 2020 due to a major LRT episode in July
395 (Sect. 3.6.1), with EC and OC increased by factors of 1.6 and 1.9, respectively compared to the mean of
396 the previous three years. For SO_4^{2-} , the increase in 2020 was only 1.25.

397 The annual mean concentration of OM (281 ± 106 ng m^{-3}) was less than for sea salt aerosol,
398 mineral dust, and even non-sea salt SO_4^{2-} , although not for all four years considered (OM > nss SO_4^{2-}
399 for 2020) (Table 2).

400 Elevated EC concentration in the H-season correspond with the AH phenomenon (Shaw, 1995),
401 and is consistent to that previously shown for eBC (Eleftheriadis et al., 2009) and SO_4^{2-} (Quinn et al.,
402 2007; Platt et al., 2022). However, three of the four highest weekly EC concentrations occurred in the
403 NH-season (Sect. 3.5). The mean EC concentration in the NH-season was five times lower than at the
404 Birkenes Observatory, and close to two orders of magnitude lower than Ispra. EC increased by a factor
405 of two during the H-season compared to the NH-season, due to more efficient transport of air masses to
406 the Arctic in winter (Ottar et al., 1989) and by AH accumulation in winter and spring (Shaw, 1995). The
407 EC level at Zeppelin in the NH-season was eight times lower than at Birkenes and nearly 60 times lower
408 than at Ispra.

409 OC levels at Zeppelin was seven times lower than at the Norwegian mainland both for the H-
410 and NH-seasons. In the H-season, levels at Zeppelin were more than 50 lower than in the polluted Po

411 Valley region, while slightly more than one order of magnitude lower in the NH-season.

412 OC seasonality (Fig. 2) was characterized by a dip in May and June, a transition period between
413 the elevated levels seen for the AH period and the mid-summer. Contemporaneous measurements of
414 organic tracers (BB, BSOA and PBAP), EC, eBC_{BB} and eBC_{FF}, largely explained the seasonality. EC
415 was elevated throughout the AH period, pointing to a dominant contribution of OC from combustion of
416 FF and BB, whereas BSOA and PBAP tracers (except for cellulose) did not start increasing until June.
417 Note that Fu et al. (2009a) found terpene oxidation products, such as 3-Methyl-1,2,3-butane-
418 tricarboxylic acid (3-MBTCA) to be elevated compared to most isoprene oxidation products during the
419 AH period at Alert (Canadian Arctic), and that only isoprene oxidation products were measured in the
420 present study. Further, results presented in section 3.5 suggest a 25% BSOA contribution to CA even in
421 winter. The BB tracer levoglucosan experienced a significant decrease from February to March,
422 suggesting that OC from fossil sources became more prominent as the AH period progressed. However,
423 we speculate that there was a substantial degradation of levoglucosan starting from the end of the polar
424 night (15 February) or as daylight hours increased, as no similar decrease was observed for eBC_{BB}. This
425 degradation might be due to factors such as aerosol particle scavenging by low-level Arctic clouds,
426 which is known to peak in early spring for BC (Zieger et al., 2023), and subsequent depletion by water
427 phase reactions. BB, BSOA and PBAP tracers typically peaked in July and August, but whereas BSOA
428 tracers decreased abruptly in early fall, PBAP tracers persisted to late fall, whereas BB tracers, EC,
429 eBC_{BB}, and eBC_{FF} started increasing again towards the end of the year.

430 Eight of the ten highest OC concentrations were observed in the NH-season, while for EC, seven
431 of the ten highest concentrations were observed in the H-season. Low emissions within the Arctic make
432 OC, and EC, seasonality susceptible to LRT episodes, and we find that the OC peak in the NH-season
433 is as strongly influenced by LRT as is EC during AH. We discuss three of these episodes in section 3.5.
434

435 **3.2 Biomass burning and fossil fuel combustion sources**

436 **3.2.1 Levoglucosan**

437 Annual mean levoglucosan concentrations ranged from 0.335 to 0.919 ng m⁻³, which is comparable to
438 the annual mean (0.680 ng m⁻³) reported for Zeppelin for March 2008 to March 2009 (Yttri et al., 2014).
439 The inter annual variability was 40%, similar to major aerosol constituents such as OC and SO₄²⁻. In
440 2020, the annual mean was twice as high as the mean of the previous three years, with an increase
441 attributed to elevated monthly means (~2 ng m⁻³) in February, July, and October (Fig. 3).

442 Increased levels and peak concentrations of levoglucosan in the H-season reflected RWC
443 emissions, as shown by Yttri et al. (2014). Increased levels in July and August were not shown by Yttri
444 et al. (2014), partly due to missing data, although impact from wild and agricultural fires was predicted
445 by modelling. In the present study, increased levels in July and August were a hallmark of the
446 levoglucosan time series, pointing to the importance of WF emissions. FLEXPART model transport of
447 modelled BC emissions also showed a substantial influence of WF emissions for July and August (2017

448 to 2020) (Fig. S1). The levoglucosan concentration in the 2020 NH-season was ~ 3-times higher than
449 the average of the three previous years, demonstrating a pronounced inter annual variability in WF
450 influence at Zeppelin. The levoglucosan to mannosan ratio (L/M) was lower for the NH-season ($4.8 \pm$
451 1.2) compared to the H-season (7.5 ± 1.9) (Fig. 3; Table S6) and might reflect a shift from WF and
452 agricultural waste burning in the NH-season to RWC in the H-season. Our findings correspond with
453 L/M ratios below 5 in summer at Gruvebadet (Ny-Ålesund) (Feltracco et al., 2020). However, we did
454 not observe the very high L/M ratios, occasionally exceeding 40, that have been attributed to emissions
455 from crops residue burning in Asia during the spring.

456

457 **3.2.2 EC_{BB} and EC_{FF} obtained from radiocarbon measurements and LHS**

458 Tracer based LHS source apportionment found that BB was the primary source of EC in all but one
459 sample (Table S3 and S4). On average, $61 \pm 15\%$ of EC was attributed to BB, with this percentage
460 varying by season: $67 \pm 5\%$ in the NH-season when EC levels were low and influenced by WF, and 57
461 $\pm 18\%$ in the H-season when RWC dominated. Our results showed a much higher BB fraction in the H-
462 season than Winiger et al. (2019) for the H-season 2012 to 2013 (36 to 39%), whereas it matched that
463 of the AH period in 2009 ($57 \pm 21\%$) (Winiger et al., 2015). The BB fraction in NH-season was slightly
464 higher than the 58 to 62% range for the NH-season in 2013 (Winiger et al., 2019). Notably, differences
465 in sample preparation and in ^{14}C analytical protocol should be considered along with inter annual
466 variability, seeking an explanation to the observed differences.

467 The weekly maximum BB fraction of EC in Feb. 2017 (81%) was somewhat lower than the
468 extremely high (95 to 98%) daily BB fractions during AH at Zeppelin in 2009 (Winiger et al., 2015).
469 Although no conclusive explanation was given to the extreme values reported by Winiger et al. (2015),
470 it cannot be excluded that that BB emissions can dominate for an entire week. eBC_{BB} apportioned by
471 PMF (Sect. 3.2.3), supports nearly exclusive (90%) BB contributions for 24 h (Fig. S2), but not for an
472 entire week (80%) (not shown). Notably, Kongsfjorden has around twenty cabins and a few research
473 stations, and wood is used for heating in these facilities when in use. Hence, emissions from these
474 sources cannot be excluded. The weekly minimum BB fraction for Jan. 2018 (21%) was much lower
475 compared to the lowest percentage reported by Winiger et al. (2015) (39%). FLEXPART footprints for
476 the Feb. 2017 and the Jan. 2018 samples were similar, covering North-West Russia and North-East
477 Greenland (not shown), providing no further insight to their extreme values, and thus “highlights the
478 complexity of BC in the Arctic atmosphere, where the generally low BC levels may be strongly
479 influenced by point sources or occasional combustion practices” (Winiger et al., 2015).

480

481 **3.2.3 eBC from biomass burning and fossil fuel combustion obtained from PMF and** 482 **FLEXPART modeling**

483 The eBC (sum of eBC_{BB} , and eBC_{FF}) and EC time series were similar, with enhanced levels during AH,
484 a small increase in mid-summer, and a slight increase towards the end of the year. FF was the major

485 fraction of eBC annually ($70 \pm 2.7\%$), in the H-season ($71 \pm 2.7\%$), and in the NH-season ($67 \pm 6.7\%$)
486 (Table 3; Fig. 4).

487 Previous modelling studies indicate that WF is the primary source of Arctic BC during summers
488 (Stohl et al., 2013; McCarty et al., 2021). ^{14}C -EC measurements support this for Zeppelin, but not for
489 other high Arctic observatories (Table 4; Winiger et al., 2019). In our study, 27% – 42% of eBC was
490 attributed to WF emissions in the NH-season, which is lower than previous findings. Our estimate
491 assumes that all eBC_{BB} in the NH-season comes from WF emissions (eBC_{WF}) and from residential wood
492 combustion emissions (eBC_{RWC}) in the H-season. Neither eBC_{WF} , nor eBC_{RWC} dominated on a monthly
493 basis (Fig. S3), although they came close in October 2017, July 2020, and October 2020, accounting for
494 46% to 48%. The annual contribution of eBC_{WF} to eBC was estimated to be 5.4% to 12%, while eBC_{RWC}
495 contributed 20 to 26%, highlighting that RWC is a larger source of eBC compared to WF.

496 FLEXPART predicted an almost equal share of BC from BB and FF annually, whereas BC_{FF}
497 ($56 \pm 3.6\%$) dominated in the H-season and BC_{BB} ($61 \pm 3.3\%$) in the NH-season (Table 3), similar to
498 results found in Stohl et al. (2013). For a direct comparison, BC_{WF} (and BC_{RWC}) was calculated similarly
499 from FLEXPART BC_{BB} output as eBC_{WF} from eBC_{BB} by PMF, i.e., BC_{WF} equals all BC_{BB} in the NH-
500 season, whereas BC_{RWC} equals all BC_{BB} in the H-season. Comparing this proxy BC_{WF} with the
501 FLEXPART modelled BC_{WF} , provided a ratio of 0.97 to 1.09 for 2017 to 2020, indicating that the BC_{WF}
502 proxy is a sound approximation. With 16 to 22% of BC attributed to WF and 27 to 36% to RWC annually
503 (Fig. 4; Table 3), FLEXPART concludes, in the same way as PMF, that $\text{RWC} > \text{WF}$, but suggests higher
504 percentages for WF and RWC fractions.

505 Neither PMF nor FLEXPART seem to fully reflect the predominant role of BC from WF above
506 50°N , which McCarty et al. (2021) suggest are larger than emissions from anthropogenic residential
507 combustion, transportation, and flaring, combined. In 2020, 56% of the BC emissions North of 65°N
508 were attributed to open biomass burning by McCarty et al. (2021), whereas 12% (PMF) and 22%
509 (FLEXPART) of (e)BC was attributed to WF at Zeppelin for 2020 in the present study. Spatial
510 variability and vertical distribution of the emissions might explain part of the discrepancy, as might mid
511 latitude emissions below 65°N , being less influenced by WF. Vertically resolved BC concentrations in
512 the Arctic in spring and summer based on aircraft measurements show a decrease with increasing altitude
513 (Jurányi et al., 2023), but this remains yet to be confirmed for BC from WF.

514 For the BB tracer levoglucosan, the fraction observed in the NH-season (36 to 64%),
515 corresponding to the WF fraction, was higher than seen for both eBC_{WF} (17 to 35%) (PMF) and BC_{WF}
516 (32 to 45%) (FLEXPART). However, degradation of levoglucosan during LRT, and lack of
517 representative (e)BC/levoglucosan ERs for a vast number of fuel categories, vegetation types, and not
518 least combustion conditions, implies considerable uncertainty in deriving the RWC/WF (e)BC split
519 using this technique.

520 Comparing PMF results to the few samples subjected to ^{14}C measurements and source
521 apportionment by tracer based LHS showed that these two approaches were on opposite ends of the

522 scale, with FLEXPART in between (Table 4). Radiocarbon measurements and LHS estimated a BB
523 fraction twice as high as the PMF approach, but all three methods agreed on a higher BB fraction in the
524 NH-season than in the H-season. Notably, BB and FF fractions of eBC derived from PMF were more
525 aligned with those from radiocarbon measurements at Zeppelin in 2012 to 2013 (Winiger et al., 2019)
526 and with fractions derived from levoglucosan measurements at Zeppelin in winter 2008 to 2009 (Yttri
527 et al., 2014). However, inter-annual variability makes such a comparison indicative only. Consideration
528 of methodological differences is essential. Crucial steps of ^{14}C -EC measurements include preventing EC
529 loss during OC removal and avoiding OC mixing with the minor EC fraction, impacting its modern vs.
530 fossil fuel signature. The advancements in the analytical approach used in this study (Rauber et al., 2023)
531 specifically aimed to improve these critical steps. Additionally, eBC derived from Aethalometer
532 measurements provides no information on the age of carbon undergoing combustion but reflects the
533 wavelength dependence of the absorption linked to the combustion condition (Garg et al., 2016.).
534 Consequently, the eBC_{FF} factor obtained by PMF could also contain emissions from combustion of
535 biofuels, observed as modern carbon by ^{14}C -measurements. Conversely, emissions from coal
536 combustion might contribute to the eBC_{BB} factor. Terms like liquid fuel instead of fossil fuel and solid
537 fuel instead of biomass burning could be more appropriate, but we maintain the notation for
538 comparability with ^{14}C -based apportionment and Aethalometer-model studies (Sandradewi et al., 2008).
539 Applying the Aethalometer-model approach with an Ångström exponent pair of (1,2) (Sandradewi et al.
540 2008) and (0.9,1.68) (Zotter et al., 2017), yields annual eBC_{BB} contributions of 32% and 29%,
541 supporting our more novel PMF approach ($27\pm 14\%$) (Table 4). Further, we note that the Ångström
542 exponents obtained from the PMF (1,1.6) are consistent with the distribution of Ångström exponents
543 observed at various sites across Europe (e.g., Tobler et al., 2021). Despite the differences in the estimated
544 contribution size from biomass vs. fossil fuel sources between ^{14}C -EC measurements and eBC by PMF,
545 important conclusions drawn are unaffected. For instance, both methods indicate the presence of
546 residential wood combustion and wildfire-sourced black carbon at Zeppelin, with a higher relative BB
547 contribution during the non-heating season.

548 Nearly exclusive (90%) contributions to eBC were seen for both eBC_{BB} and eBC_{FF} for periods
549 of 24 h (Fig. S2, upper left panel). This corresponds with 24 h ^{14}C -EC data from Zeppelin dominated
550 (EC $f_{\text{bb}} > 95\%$) by contemporary carbon (Winiger et al., 2015), and ^{14}C -EC data dominated (EC $f_{\text{ff}} >$
551 95%) by fossil carbon observed at other high Arctic sites (Winiger et al., 2019). Exclusive contributions
552 were most frequent for eBC_{FF} and seen for 1.1% of the dataset compared to 0.1% for eBC_{BB} . Hence,
553 with a few exceptions, eBC_{BB} and eBC_{FF} co-appear.

554

555 **3.3 Biogenic secondary organic aerosol - 2-methyltetrols**

556 2-methyltetrols (here: sum of 2-methylerythritol and 2-methylthreitol) are primarily formed from the
557 acid-catalyzed multiphase chemistry of isoprene epoxydiols (IEPOX) (Surratt et al., 2010; Lin et al.,
558 2012; Cui et al., 2018), which are important low- NO_x oxidation products of isoprene (Paulot et al.,

559 2009), the biogenic volatile organic compound (500 Tg C yr⁻¹) emitted in highest amount globally
560 (Williams and Koppmann, 2007), and an important source of BSOA (Hallquist et al., 2009; Noziere et
561 al., 2015). Their low-level presence in the Arctic has been demonstrated in only a few studies covering
562 a few months (e.g., Fu et al., 2009a). We discuss their level, seasonality, sources, and LRT vs. local
563 formation over four consecutive years.

564 2-methyltetrol concentrations at Zeppelin were at the lower range of those reported in Europe
565 (Ion et al., 2005; Kourtchev et al., 2005; 2008 a,b), North-America (Cahill et al., 2006; Xia and Hopke;
566 200; Cui et al., 2018), South-America (Claeys et al., 2010) and Asia (Fu et al., 2010), and consistent
567 with levels observed at Alert in the Canadian Arctic (Fu et al., 2009a). The duration of the elevated 2-
568 methyltetrols concentrations during the peak of the inter annual cycle at Zeppelin appears quite like that
569 at the Birkenes Observatory (Southern Norway) 2300 km further south: with an onset in June and peak
570 concentrations in July and August, the time series at Zeppelin is delayed by half a month compared to
571 Birkenes (Fig. 6 in Yttri et al., 2021), although concentrations drop by mid-October at both sites. The
572 annual mean 2-methyltetrols concentration was 3 times lower at Zeppelin compared to Birkenes in 2017
573 and 5 in 2018. In 2019, the 2-methyltetrol level at Zeppelin increased by a factor of three compared to
574 2017 to 2018 and in 2020 by a factor of nine, and thus for 2020 the annual mean at Zeppelin (1.15 ng
575 m⁻³) was nearly twice as high as the highest annual mean seen at Birkenes (0.610 ng m⁻³ in 2018).

576 The atmospheric lifetime of isoprene is < 4 hours, whereas the lifetime of 2-methyltetrols is
577 unknown (Wennberg et al., 2018) and the amount attributed to formation from locally emitted isoprene
578 vs. LRT 2-methyltetrols remains an open question. The 2-methyltetrols level at Birkenes increase by
579 nearly a factor of 20 when leaves unfold in May (Yttri et al., 2021). Consequently, the effect of leaves
580 unfolding 0.5 to 1.5 months earlier in continental Europe (the leaves of *Betula Pubescens* unfold 2.1
581 days later pr. 100 km along a South to North transect in Europe; Rötzer and Chmielewski, 2001) does
582 not seem to have an influence, suggesting that the 2-methyltetrols level largely reflect local formation.
583 At Svalbard, there are no forests, and hardly any trees, still there is vegetation (including mosses and
584 lichens) that emit isoprene, that can have emission rates that are considerably higher than those observed
585 at Southern latitudes (Kramshøj, et al., 2016). Circumpolar land masses are situated further away from
586 Zeppelin than continental Europe from Birkenes, thus local formation of 2-methyltetrols might be
587 important also at Svalbard. Marine sources of isoprene cannot be excluded, particularly in remote marine
588 areas (Liakakou et al., 2007), although macro algae seem to favor dimethyl sulfide (DMS) formation
589 rather than isoprene in the Arctic (Dani and Loreto, 2017). Further, time series of 2-methyltetrols and
590 MSA at Zeppelin (Sharma et al., 2012) do not co-vary, suggesting a non-marine origin of 2-
591 methyltetrols.

592 The increased 2-methyltetrol level at Zeppelin in 2019 to 2020 occurred during summer. From
593 30 June to 11 of August 2020, weekly mean concentrations ranged from 5.9 to 28 ng m⁻³ for four out of
594 six weeks, being up to five times higher than the highest weekly mean at Birkenes (5.6 ng m⁻³) for 2017
595 to 2018. We recognize that levoglucosan was elevated (1.0 to 6.0 ng m⁻³) for these four weeks and that

596 air masses were influenced by WF emissions in Western Russia (Fig. 7; Sect. 3.5.1). We are left
597 speculating how WF might have augmented 2-methyltetrol levels. Isoprene emissions are enhanced by
598 increased temperature and a fire plume provides favorable conditions for BSOA formation and aerosol
599 surface area for condensation. Notably, 2-methyltetrols are semi volatile (Lopez-Hilfiker et al., 2016)
600 and at high OA loadings increased partitioning to the aerosol phase will occur. Further, transport time
601 was short (Fig. S3), which is favorable concerning potential degradation of 2-methyltetrols. Increased
602 formation from local isoprene emissions is likely, as ambient temperature at Zeppelin was
603 unprecedentedly high in this period (See Sect 3.5.1 and Fig. 7 for details). The elevated 2-methyltetrol
604 concentration (3.7 ng m^{-3}) seen for the warm period in the beginning of July 2019 was not nearly as high
605 as for July and August 2020 and levoglucosan (0.04 ng m^{-3}) was not increased.

606 2-methyltetrols (here: ng C m^{-3}) contributed up to 0.34% to OC monthly in the NH-season in
607 2019 and 0.56% in 2020, being clearly higher compared to the two previous years (0.14% and 0.23%),
608 which in turn was higher than the highest monthly means at Birkenes (0.09% and 0.12%). Compared to
609 rural central Europe (0.68% in June) (Ion et al., 2005) and Boreal Forest Finland (0.88% in the July to
610 August transition) (Kourtchev et al., 2005), the highest contributions at Zeppelin in 2020 are slightly
611 lower.

612 Multi-year time series of 2-methyltetrols are rare, particularly in areas with low NO_x -
613 concentrations (Noziere et al., 2011; Cui et al., 2018). We find that the NH-season drop in the 2-
614 methylthreitol to 2-methylerythritol ratio was much more pronounced at Birkenes (0.36 ± 0.11) than at
615 Zeppelin (0.54 ± 0.12) (Table S6). A NH-season drop is also observed the Hyytiälä Observatory (Boreal
616 Forest Finland) (Kourtchev et al., 2005). Elevated ratios were observed at Zeppelin in July (0.83) and
617 August (0.70) 2020 when influenced by WF emissions, being substantially higher compared to July –
618 August (0.45 ± 0.04) of previous years. With the exceptions mentioned, the mean ratio for the NH-
619 season at Zeppelin agrees with the upper range (0.25 to 0.58) reported by others (Claeys et al., 2010).
620 This relates to the formation mechanism of 2-methyltetrols outlined by Bates et al. (2014), which shows
621 a 1:2 relationship between *cis*- β -IEPOX and *trans*- β -IEPOX, accounting for >97% of observed IEPOX,
622 and which are the precursors of 2-methylthreitol and 2-methylerythritol, respectively. Notably, 2-
623 methyltetrols can also result from the degradation of IEPOX-derived organosulfates through hydrolysis
624 of tertiary ones (Darer et al., 2011), however these species were not measured in the present study.

625 There are studies suggesting a biological (enzymatic) origin of 2-methyltetrols, as there is an
626 enantiomer excess of both 2-C-methyl-D-erythritol and 2-C-methyl-threitol (Noziere et al., 2011;
627 González et al., 2014; Jacobsen and Anthonsen, 2015). If the 2-methyltetrols formation was exclusively
628 abiotic, resulting from atmospheric oxidation of isoprene (Claeys et al., 2004), there would be a racemic
629 mixture of the 2-methyltetrols. This is consistent with the known production of the 2-methylerythritol
630 D-form by plants, algae, and microorganisms (Anthonsen et al., 1976, 1980; Dittrich and Angyal, 1988;
631 Ahmed et al., 1996; Duvold et al., 1997; Sagner et al., 1998; Enomoto et al., 2004). Consequently, it can
632 be questioned if 2-methyltetrols are exclusive tracers of BSOA from atmospheric oxidation of isoprene,

633 e.g., a 30 to 67% biological contribution was calculated for May to December for the Aspvreten site
634 (Sweden) (Noziere et al., 2011). Unfortunately, the analysis done in the present study does not allow for
635 a proper investigation of a potential biological contribution. Cahill et al. (2006) argued for a biological
636 source based on the correlation between 2-methyltetrol and the PBAP tracers glucose ($r^2 = 0.732$) and
637 fructose ($r^2 = 0.644$) for eleven samples. At Zeppelin, r^2 for 2-methyltetrols vs. fructose (0.951), glucose
638 (0.946) and arabitol (0.801) appears elevated in the NH-season but drops substantially ($r^2 = 0.052 -$
639 0.437) when excluding the extreme values in July and August 2020. At Birkenes, correlation was non-
640 existing ($r^2 = 0.000 - 0.025$). Source apportionment of CA by PMF at Birkenes showed that the factor
641 explaining 94% of the 2-methyltetrols explained only 6% of the PBAP tracers, and that the factor
642 explaining 89% of the PBAP tracers explained only 2.5% of the 2-methyltetrols (Yttri et al., 2021).
643 Hence, statistics do not argue for a common source of 2-methyltetrols, or a fraction of 2-methyltetrols,
644 and PBAP tracers. Further, 2-methylerythritol vs. 2-methylthreitol correlated highly both at Zeppelin (r^2
645 $= 0.971$) and at Birkenes ($r^2 = 0.889$), suggesting one dominating source (abiotic secondary formation),
646 corresponding to findings by El-Haddad et al. (2011). However, potential mechanisms by which
647 biologically formed 2-methyltetrols are released to the atmosphere are not known, thus a biological
648 contribution cannot be excluded.

649

650 **3.4 Primary biological aerosol particles**

651 The interest in PBAP has grown over the last two decades, with rising awareness of its contribution to
652 the OA budget (e.g., Waked et al. 2014; Yttri et al. 2021; Moschos et al., 2022) and as a source of warm
653 ice nucleating particles, deemed more important than cloud condensation nuclei regarding Arctic cloud
654 radiative properties (Solomon et al., 2018). We address a handful of PBAP tracers, discuss their levels,
655 seasonality, and sources, including cellulose, measured in Arctic aerosol for the first time.

656

657 **3.4.1 Sugars and sugar-alcohols**

658 Annual mean concentrations of sugars and sugar-alcohols were 1 to 2 orders of magnitude lower at
659 Zeppelin compared to Birkenes, reflecting the modestly vegetated Arctic and that PBAP mainly have a
660 local origin (Samaké et al., 2019). This contrasts with the factors for 2-methyltetrols (≤ 5), which are
661 secondarily formed species with a stronger regional character but might also relate to the temperature
662 sensitive high flux of biogenic volatile organic compounds for Arctic vegetation (Kramshøj et al., 2016).
663 Higher levels of primary biological organic aerosol (PBOA) at Gruvebadet (50 m asl), one km south of
664 Ny-Ålesund, compared to the Zeppelin Observatory (472 m asl) (Moschos et al., 2022) indicate a local
665 contribution associated with the more verdant lower altitude areas. However, maximum concentrations
666 of sugars and sugar-alcohols were observed for the LRT episode 22 – 27 July 2020 (Sect. 3.6.1),
667 explaining 29% of the annual sugars and sugar-alcohols loading. We are left speculating about the LRT
668 fraction of PBAP vs. that of local origin, but LRT likely makes a larger contribution to PBAP in the
669 Arctic than for more vegetated southerly biomes.

670 All species experienced a modest increase in June, coinciding with the onset of the growing
671 season, but evolved differently after that, suggesting a mixture of sources, highlighting the importance
672 of measuring a broad spectrum of PBAP tracers. Arabitol and mannitol were elevated throughout
673 summer before successively declining towards the end of the year, fructose and glucose started
674 decreasing immediately after the peak level in July, whereas trehalose experienced comparable levels
675 from July to November. Snow cover can be decisive for PBAP levels (Yttri et al., 2007 a, b) and probably
676 more so for the non-forested Arctic. However, our data does not explicitly demonstrate an influence of
677 the snow cover, e.g., the seasonality of trehalose (and cellulose; Sect 3.4.2).

678 The composition of sugars and sugar-alcohols at Zeppelin (Table 1) and Birkenes (Table S5)
679 varied, reflecting different biomes. Glucose was the most abundant sugar regardless of the season at
680 Zeppelin. At Birkenes, glucose dominated only in winter, while arabitol and mannitol were more
681 prominent in summer. Trehalose levels were comparable or slightly higher than arabitol and mannitol
682 at Zeppelin but lower at Birkenes. Samaké et al. (2020) showed how only a few genera of fungi and
683 bacteria were responsible for the sugar and sugar-alcohol containing PBAP in PM₁₀ filter samples at a
684 rural site in France, and that these were associated with leaves rather than soil material. This strong
685 association between sugars and sugar-alcohols and vegetation likely explain the very low levels of these
686 PBAP tracers at Zeppelin compared to Birkenes. Samaké et al. (2020) point to the fungus *Cladosporium*
687 *sp.* when explaining ambient aerosol levels of arabitol, mannitol and trehalose, as does Yttri et al.
688 (2007a) for Birkenes. The annual mean mannitol to arabitol ratio was comparable between Zeppelin (1.1
689 ± 0.5) and Birkenes (1.0 ± 0.0) (Table S6), and to values reported for the Nordic countries (Yttri et al.,
690 2011b). Mannitol and arabitol were highly correlated in the NH-season ($r^2 = 0.983$) when levels were
691 elevated, and mannitol to arabitol ratio variability minor, suggesting one common source dominating.
692 However, four samples with a mannitol to arabitol ratio ≥ 3 in the April to May transition could indicate
693 influence from another source. Mannitol is considered the most abundant naturally occurring polyol,
694 present and produced in a wide range of living organisms (Tonon et al., 2017), accounting for 25% of
695 the dry weight of macro algae for certain parts of the year (Horn et al., 2000), however, our data for
696 Zeppelin suggest that fungal spores are decisive for arabitol and mannitol present in the Arctic aerosol.
697 Assuming all mannitol was associated with fungal spores, their carbon content contributed $0.5 \pm 0.2\%$
698 to OC annually when applying the lower OC/mannitol ratio (5.2) of Bauer et al. (2002), whereas the
699 highest monthly mean was seen for September ($1.5 \pm 1.2\%$). The contribution reached 5% for only two
700 of the weekly samples. Using the higher OC/mannitol ratio (10.8), would double these estimates.

701 Glucose is a building block of natural dimers and polymers and a ubiquitous primary molecular
702 energy source, and thus an important PBAP. Small amounts of glucose are present in RWC emissions
703 (Nolte et al., 2001) and are increased in air masses influenced by forest fire smoke (Medeiros et al.,
704 2006). Notably, nine of the ten samples highest in glucose were also highly increased with respect to
705 levoglucosan and were all collected in the NH-season (Table S8), demonstrating WF as an important
706 source of glucose brought to the Arctic by LRT. A largely similar finding was made for the other sugars

707 and sugar-alcohols. Previous studies do not seem to link fungal related sugars and sugar-alcohols
708 (arabitol, mannitol, trehalose) with WF emissions (e.g., Table 5 in Medeiros et al., 2006), nor with RWC
709 emissions, e.g., levoglucosan and sugar-alcohols end up in different factors in PMF studies (Waked et
710 al., 2014; Yttri et al., 2021). This might partly be due to lack of correlation between levoglucosan and
711 sugar-alcohols for an entire data set. Indeed, low correlations between levoglucosan and sugar-alcohols
712 ($r^2_{\text{NH-season}} < 0.423$; $r^2_{\text{H-season}} < 0.056$) were obtained considering the entire data set for Zeppelin, although
713 the data presented in Table S8 clearly demonstrates a connection between WF and sugar-alcohols.

714 We estimated a 7 – 15% contribution of PBAP to OC annually, using an OC-to-PBAP_{Tracers}
715 emission ratio (ER) of 14.6 ± 2.1 (Zwaafink et al., 2022), derived from measurements in the Boreo-
716 nemoral zone (Yttri et al., 2021), keeping in mind that such an ER would be site specific.

717 718 **3.4.2 Cellulose**

719 Cellulose was the most abundant organic tracer analyzed (annual mean concentration of $2.2 \pm 0.6 \text{ ng m}^{-3}$)
720 ³), but levels were much lower than in rural areas of continental Europe (annual mean: $16.3 - 284 \text{ ng m}^{-3}$)
721 ³) (Sánchez-Ochoa et al., 2007; Brighty et al., 2022), likely due to sparse vegetation at Svalbard. The
722 highest monthly means were seen for June followed by October, but there was no pronounced
723 seasonality for cellulose as seen for the other PBAP tracers (Sect. 3.4.1). This corresponds with findings
724 made by Sánchez-Ochoa et al. (2007) who pointed to a minor seasonality “*with higher winter levels*
725 *than expected*”, and that of Puxbaum and Tenze-Kunit (2003) who associated increased cellulose levels
726 in spring with “*seed production and repulsing of other cellulose containing plant material*”, and
727 “*production of leaf litter*” in fall. High wind speed might be a driving force for generation and
728 entrainment of cellulose containing aerosol particles that is more pronounced in winter, and particularly
729 in the harsh Arctic climate, but possibly limited by snow cover. In the recent study by Brighty et al.
730 (2022), a clear seasonality was shown with increased levels in summer and fall at French and Swiss
731 rural sites.

732 Size distribution measurement of cellulose is limited and inconclusive, with highest
733 concentrations reported both for the fine (Puxbaum and Tenze-Kunit, 2003) and the coarse mode (Yttri
734 et al., 2011a; Brighty et al., 2022). Lack of comparable seasonality between nearby sites indicates that
735 local sources dominate (Brighty et al., 2022), but with a certain fraction associated with fine aerosol,
736 LRT is a possibility. Cellulose did not correlate with other PBAP tracers or levoglucosan, corresponding
737 to the findings by Brighty et al. (2022), but this does not exclude co-emission (see Sect. 3.4.1). A minor
738 fraction (0.08%) of RWC emissions was attributed to cellulose in a combustion study by Schmidl et al.
739 (2008), but we found no strong connection between the samples highest in cellulose and levoglucosan,
740 as we did for the other PBAP tracers and levoglucosan, nor between cellulose and the other PBAP tracers
741 (Table S8). The lack of resemblance between cellulose and other PBAP tracers and BB aerosol should
742 be explored further.

743 Cellulose (here: ng C m^{-3}) made a $1.0 \pm 0.3\%$ contribution to OC annually, corresponding to the

744 lower range reported for rural background sites along an east to west transect across Europe (0.7 – 3.9%)
745 (Sánchez-Ochoa et al., 2007), but substantially lower compared to French ($3.2 \pm 2.4\%$) and Swiss
746 ($5.9 \pm 4.4\%$) rural background sites (Brighty et al., 2022).

747 The contribution of plant debris (here: ng C m^{-3}) was estimated from cellulose (Puxbaum and
748 Tenze Kunit, 2003; Yttri et al., 2011a,b) as a $2.0 \pm 0.6\%$ contribution to OC annually, and thus somewhat
749 higher than for fungal spores (0.5 – 1.1%). On a monthly basis, 4 to 6% contributions were observed in
750 all seasons. Weekly samples ($n = 23$) with a high (5 to 12%) plant debris contribution were associated
751 with low OC levels (mean: 53 ng C m^{-3} ; 22 percentile). Plant debris and OC were correlated ($r^2 = 0.707$),
752 suggesting that plant debris is a driver of observed OC levels at low concentrations. We did not observe
753 a similar feature for fungal spores.

754

755 **3.5 Source apportionment of carbonaceous aerosol by Latin Hypercube Sampling**

756 Source apportionment of CA (here: TC) by the LHS approach showed that natural sources dominated
757 in the NH-season (85%) and anthropogenic in the H-season (73%), assuming all biomass burning
758 emissions originated from WF in the NH-season and from RWC in H-season (Fig. 5). Even without
759 attributing BB emissions to WF, natural sources still dominated in the NH-season (60%).

760 BSOA (56%) was the most abundant natural source in the NH-season, then WF (26%) and
761 PBAP (3.2%). Compared to previous studies (Yttri et al., 2011 a and b), we found a lower PBAP
762 fraction, which we attributed to the less vegetated Arctic environment. Note that the LHS approach
763 underestimate the PBAP fraction by only accounting for fungal spores and plant debris, apportioning a
764 part of PBAP to BSOA (Yttri et al., 2021). The PBAP fraction increased to 11% when using an OC-to-
765 $\text{PBAP}_{\text{Tracers}}$ emission ratio (ER) of 14.6 ± 2.1 (Zwaafink et al., 2022) including the sum of arabinol,
766 mannitol, glucose, and trehalose. Note that this ER was obtained from measurements in the boreo-
767 nemoral zone, and thus more representative of LRT than local PBAP sources.

768 RWC (46%) was the major fraction in the H-season followed by FF (27%) and BSOA (25%),
769 whereas PBAP (1.4%) was negligible, even when considering the upper estimate (2.7%) obtained using
770 the ER by (Zwaafink et al., 2022). The absence of 2-methyltetrols in winter indicated that BSOA was
771 formed from oxidation of mono- and sesquiterpenes and dimethyl sulfide, which seem more abundant
772 in the Arctic winter than oxidation products of isoprene (Fu et al., 2009a; Sharma et al., 2012). Further,
773 modelling studies suggest that increased condensation may explain wintertime BSOA (Simpson et al.,
774 2007), which might be particularly relevant for the low Arctic temperatures.

775 Our source apportionment results for Zeppelin aligns with findings from rural background sites
776 in Europe (e.g., Gelencsér et al., 2007; Genberg et al., 2011; Gilardoni et al., 2011; Glasius et al. 2017;
777 Yttri et al., 2011a), where RWC dominates during the H-season and BSOA dominate in the NH-season.
778 Rerunning the analysis using levoglucosan instead of $^{14}\text{C-EC}$ for apportionment of BB emissions,
779 lowered the contribution from WF in the NH-season from 26% to 4.4%. However, the contribution from
780 natural sources remained consistent, as BSOA accounted for the modern carbon redistributed from WF.

781 In the H-season, the contribution from RWC decreased from 46% to 8.9%, making BSOA (62%) and
782 natural sources (64%) the major fractions even in the H-season. Hence, the choice of tracer
783 (levoglucosan vs. ^{14}C -EC) would lead to different results and conclusions for Zeppelin.
784

784

785 **3.6 LRT episodes outside the AH period**

786 LRT episodes are decisive for CA levels and seasonality observed at Zeppelin. We analyzed in detail
787 the three episodes with the highest weekly means of OC, which also had three of the four highest weekly
788 means of EC (Figs. 6 to 8). All these episodes had air masses originating from NW Eurasia.
789

789

790 **3.6.1 Episode 1 (22 July to 27 July 2020) – WF, BSOA, and PBAP**

791 In transition July to August 2020, CA levels were high, with peak concentrations from 22 – 27 July
792 (2172 ng C m^{-3} for OC and 59 ng C m^{-3} for EC). These levels were the highest in four years of
793 observations, explaining 21% of the annual OC loading, but only 7% of EC. However, levels were still
794 lower than the record high concentrations ($3.5 \mu\text{g C m}^{-3}$ for OC and $0.24 \mu\text{g C m}^{-3}$ for EC) observed in
795 the April to May transition 2006, caused by emissions from wild and agricultural fires in Eastern Europe
796 (Stohl et al., 2007). All tracers (except cellulose) experienced maximum values during this episode, but
797 2-methyltetrols, glucose, fructose, and arabitol were the most elevated when compared to the long-term
798 annual mean and to the enhancement seen for OC. The FLEXPART footprint clearly shows an influence
799 from WF in the Khanty-Mansi district (Western Russia) (Fig. 7), corroborating to the high levoglucosan
800 concentration (6.0 ng m^{-3}). Source apportionment by PMF attributed 55% of eBC to BB, whereas
801 FLEXPART calculated 62%, with WF (95%) as the totally dominating fraction. Flaring was the
802 dominating fossil fuel source category according to FLEXPART, explaining 58% of BC from fossil fuel
803 sources.

804 The plume transport time from the source region to the Zeppelin Observatory was short; less
805 than 7 days for 67% of eBC observed at Zeppelin 25 to 27 of July (Fig. S3), whereas on average only
806 30% of the observed eBC reaches the Arctic station after such short time. This might have contributed
807 to the high level of 2-methyltetrols, which are indicated to have short atmospheric lifetimes (Yttri et al.,
808 2021), in addition to the arguments raised in section 3.3. Certain PBAP, such as fungal spores (Bauer et
809 al., 2002; Yttri et al., 2007a) are small enough to be transported over long distances, even between
810 continents (Prospero et al., 2005), and pyro convection might bring larger sized PBAP to altitudes that
811 enables LRT (e.g., Zwaafink et al., 2022). PBAP contributed 14% of OC, using the $\text{OC-to-PBAP}_{\text{Tracers}}$
812 ER by Zwaafink et al. (2022).

813 The high CA level coincided with a prolonged period (24 to 29 July) of high temperatures,
814 unprecedented since temperature measurements were initiated at Zeppelin (1998), caused by intrusions
815 of warm air masses from Siberia; $T > 10 \text{ }^\circ\text{C}$ for 111 consecutive hours, mean $T = 14.5 \pm 1.5 \text{ }^\circ\text{C}$, and
816 $T_{\text{Max}} = 18.2 \text{ }^\circ\text{C}$. A disproportionally strong warming of the Arctic compared to the midlatitudes could
817 create an important pathway of pollution to the Arctic (Stohl et al. 2007), and as for the LRT episode in

818 spring 2006 (Stohl et al., 2007), emissions from WF at lower latitudes were essential in the deterioration
819 of Arctic air quality also in July 2020.

820

821 **3.6.2 Episode 2 (28 Sep to 6 Oct 2017) – A bit of everything**

822 Air masses with a history over south-western Russia, eastern, central, and northern Europe (including
823 Scandinavia) (Fig. 8) increased the OC (549 ng C m^{-3}) and EC (52 ng C m^{-3}) concentrations at Zeppelin
824 to levels corresponding to 14% of their annual loading. Source apportionment by the LHS suggested
825 that BSOA (57%) and BB (32%) dominated CA (Table S4). Certain PBAP tracers (arabitol, mannitol
826 and trehalose) were enhanced beyond that of OC, reflecting the seasonal peak in fungal spores, but
827 PBAP contributed only 3% to CA (Table S4). An upper estimate of 13% was obtained using the OC-to-
828 $\text{PBAP}_{\text{Tracers}}$ ER by Zwaafink et al. (2022). PMF apportioned 47% of eBC to BB, comparing well with
829 FLEXPART (51%), (ascribing 62% of BB to WF) and LHS (58%). FLEXPART apportioned the
830 majority of BC from FF combustion to traffic (55%). The mean ambient temperature during the episode
831 was enhanced compared to the long-term mean, as seen for all three episodes described.

832

833 **3.6.3 Episode 3 (2 to 10 Oct 2020) – Wildfires and mineral dust**

834 This episode was studied by Zwaafink et al. (2022), combining surface and remote sensing
835 observations and transport model simulations to understand its origin and development, whereas we in
836 the present study focused on its carbonaceous aerosol content. Briefly, the EC level (78 ng C m^{-3}) was
837 the highest in four years of observations, whereas the OC level (818 ng C m^{-3}) was much lower than
838 observations made during the July 2020 (Sect 3.5.1) episode, explaining 15% and 13% of the annual
839 EC and OC loading, respectively (Fig. 9). Levoglucosan (5.0 ng m^{-3}) was the only organic tracer
840 elevated beyond that of OC, supporting FLEXPART calculations pointing to WF emissions in Ukraine
841 and southern Russia, as one of two major sources of air pollution for this episode. Source
842 apportionment of eBC by PMF indicated an almost equal share of eBC from BB (52%) and FF
843 combustion (48%), as do FLEXPART (BB = 57% and FF = 43%), with the majority of BB attributed
844 to WF (72%), and traffic being the major FF category (52%). Mixing with mineral dust emissions
845 from Central Asia en route, caused a mineral dust level of $1.9 - 2.6 \mu\text{g m}^{-3}$, likely explaining the
846 presence of carbonate (20 ng C m^{-3} ; $100 \text{ ng CO}_3^{2-} \text{ m}^{-3}$). Before entering the Arctic, the polluted air
847 masses deteriorated the air-quality in a large part of northern Europe, giving PM_{10} levels around 100
848 $\mu\text{g m}^{-3}$, and the same aerosol particle chemical signature as described for Zeppelin. These levels violate
849 EU air quality guidelines, which have daily mean limit values for PM_{10} of $50 \mu\text{g m}^{-3}$.

850

851 **4 Implications**

852 Lack of long-term OA measurements has been a limitation for understanding Arctic aerosol mass
853 closure. Further, OA speciation needed for source attribution and for studying impact on cloud
854 condensation nuclei and ice nucleating particles are scarce. Our four-years study at Zeppelin

855 Observatory at Svalbard shed light on some of these topics, demonstrating that OA is a significant
856 fraction of the Arctic PM₁₀ aerosol particle mass, though less than sea salt aerosol and mineral dust, as
857 well as typically non-sea salt SO₄²⁻. LRT episodes in the non-heating season dominated by natural
858 emissions and their impact on OA levels, seasonality, and composition received particular focus,
859 showing that WF also contribute to high BSOA and PBAP levels in the Arctic environment. The fraction
860 of OA attributed to local sources vs. LRT is uncertain, particularly when experiencing intrusions of
861 warm air masses from Siberia, as certain Arctic vegetation species have highly temperature sensitive
862 biogenic volatile organic compounds emission rates. Arctic CA shares the same feature as CA in source
863 regions in the mid latitudes (e.g., Gelencsér et al., 2007), i.e., natural sources, particularly BSOA,
864 dominating in the non-heating season and anthropogenic emissions, predominantly RWC, in the heating
865 season. The nine-fold increase in 2-methyltetrols observed for 2020 could be a harbinger of CA from
866 natural sources increasing in the Arctic.

867 Contrary to both previous (Stohl et al., 2013; Winiger et al., 2019) and present (this study)
868 modeling and radiocarbon studies, PMF did not predict WF as the major source of eBC at Zeppelin
869 Observatory in the non-heating season. However, the predominant role of BC from WF emissions at
870 Northern latitudes stated by McCarty et al. (2021) was neither reflected by PMF nor by FLEXPART for
871 2017 to 2020. This calls for an investigation of whether the stated increase in BC from WF emissions
872 for 2010 – 2020 at Northern latitudes (McCarty et al., 2021) is reflected at Arctic ground level. Up to
873 two decades of stored multi wavelength aethalometer data for Arctic observatories, combined with the
874 outlined PMF approach enables such a trend study. Additionally, a pan-Arctic investigation is
875 encouraged for studying the spatial variability in eBC_{BB} and eBC_{FF}, facilitated by the inexpensive, high
876 time resolution multi wavelength Aethalometer measurements that are widespread across the Arctic
877 observatories (EU Action on Black Carbon in the Arctic, 2019). Increased anthropogenic activity such
878 as shipping oil and gas exploration in the Arctic, warrants further separation of eBC from FF combustion,
879 which can be attempted using additional high time resolution data as input to our analysis. This appears
880 particularly important for the flaring source, suggested by modelling to contribute 42% to the annual
881 mean BC surface concentration in the Arctic (Stohl et al., 2013), which yet remains to be confirmed by
882 observations.

883 Our study shows a wide variability amongst different methods in apportioning BC according to
884 FF and BB, warranting further investigation for a reliable abatement of sources relevant for BC in the
885 Arctic. Still, the high time resolution observational signal of eBC from BB and FF combustion derived
886 from Aethalometer measurements provide a hitherto unused tool important for assessing Arctic BC.

887 Continuation of the actual time series at Zeppelin Observatory is suited for revealing potential
888 changes in the relative source composition of Arctic CA, be it from altered transport or changes in
889 emissions. It is of special interest to monitor the frequency and magnitude of WF, how BSOA and PBAP
890 concentrations develop, and if FF emissions change from increased anthropogenic activity in the Polar
891 region.

892
893
894
895
896
897
898
899
900
901
902
903
904
905
906
907
908
909
910
911
912
913
914
915
916
917
918
919
920
921
922
923
924
925
926
927
928
929
930
931

Data availability

All data used in the present paper are open access and are available at <http://ebas.nilu.no/> (NILU, 2023), except radiocarbon data, which are presented in Rauber et al. (2023).

Supplement

The supplement related to this article is available online at:

Author contributions

SMP, KEY, and WA were responsible for conceptualizing the study. KEY wrote the original draft of the paper. WAA, SE, and KEY produced the figures. AB was responsible for collection of aerosol filter samples. HG analysed the organic tracers, MR and SS did the radiocarbon measurements, and AK-G was responsible for the cellulose analysis. MF, KEY, CLM, and WA carried out data curation. NE and SE did the FLEXPART modelling, whereas DS and MAY did the LHS calculations. SMP and KEY undertook the formal analysis. JS, AG, and ZZ acquired resources. KT, CLM and WA acquired funding. All co-authors contributed to writing, reviewing, and editing the final article.

Competing interests:

The contact author has declared that none of the authors has any competing interests.

Acknowledgement

The Norwegian Ministry of Climate and Environment provided funding to establish the OC/EC and organic tracers time series used in the present study and are gratefully acknowledged. These data are reported to the EMEP monitoring programme and are available from the EBAS database infrastructure (<http://ebas.nilu.no>) hosted at NILU. The research leading to these results has benefited from the Aerosols, Clouds, and Trace gases Research InfraStructure (ACTRIS) network, funding from the European Union Seventh Framework Programme (FP7/2007–2013) under ACTRIS-2 and grant agreement no. 262254 (i.e., participation in inter-laboratory comparison for thermal–optical analysis and QA and QC of measurements. S.E. and N.E. received funding from AMAP and the ABC-iCAP project. Staff from the Norwegian Polar Institute are greatly acknowledged for changing of filters at the Zeppelin Observatory. A.G., Z.Z. and J.D.S. thank the US National Science Foundation (NSF) under Atmospheric and Geospace (AGS) Grant 2001027 for funding the synthesis of 2-methyltetrols used in this study. We used ChatGPT (3.5) to condense and improve the language of specific sections in the review process of this manuscript.

Financial support.

This research has been supported by the Norwegian Ministry of Climate and Environment.

References

- 932 Aas, W., Eckhardt, S., Fiebig, M., Solberg, S., and Yttri, K. E.: Monitoring of long-range transported
933 air pollutants in Norway, annual report 2019, Miljødirektoratet rapport, NILU, Kjeller, Norway, M-
934 1710/2020 NILU OR 4/2020, 2020.
- 935 Agrios, K., Salazar, G., Zhang, Y. L., Uglietti, C., Battaglia, M., Luginbuhl, M., Ciobanu, V. G.,
936 Vonwiller, M., and Szidat, S.: Online coupling of pure O-2 thermo-optical methods-C-14 AMS for
937 source apportionment of carbonaceous aerosols, *Nuclear Instruments & Methods in Physics Research*
938 *Section B-Beam Interactions with Materials and Atoms*, 361, 288-293, 10.1016/j.nimb.2015.06.008,
939 2015.
- 940 Ahmed, A. A., AbdElRazek, M. H., AbuMostafa, E. A., Williams, H. J., Scott, A. I., Reibenspies, J. H.,
941 and Mabry, T. J.: A new derivative of glucose and 2-C-methyl-D-erythritol from *Ferula sinaica*, *Journal*
942 *of Natural Products*, 59, 1171-1173, 1996.
- 943 Akagi, S. K., Yokelson, R. J., Wiedinmyer, C., Alvarado, M. J., Reid, J. S., Karl, T., Crouse, J. D., and
944 Wennberg, P. O.: Emission factors for open and domestic biomass burning for use in atmospheric
945 models, *Atmospheric Chemistry and Physics*, 11, 4039-4072, 10.5194/acp-11-4039-2011, 2011.
- 946 Alastuey, A., Querol, X., Aas, W., Lucarelli, F., Perez, N., Moreno, T., Cavalli, F., Areskoug, H., Balan,
947 V., Catrambone, M., Ceburnis, D., Cerro, J. C., Conil, S., Gevorgyan, L., Hueglin, C., Imre, K., Jaffrezo,
948 J.-L., Leeson, S. R., Mihalopoulos, N., Mitisinkova, M., O'Dowd, C. D., Pey, J., Putaud, J.-P., Riffault,
949 V., Ripoll, A., Sciare, J., Sellegri, K., Spindler, G., and Yttri, K. E.: Geochemistry of PM₁₀ over Europe
950 during the EMEP intensive measurement periods in summer 2012 and winter 2013, *Atmospheric*
951 *Chemistry and Physics*, 16, 6107-6129, 10.5194/acp-16-6107-2016, 2016.
- 952 Anthonsen, T., Hagen, S., Kazi, M. A., Shah, S. W., and Tagar, S.: 2-C-methyl-erythritol, a new
953 branched alditol from *convolvulus-glomeratus*, *Acta Chemica Scandinavica Series B-Organic*
954 *Chemistry and Biochemistry*, 30, 91-93, 10.3891/acta.chem.scand.30b-0091, 1976.
- 955 Anthonsen, T., Hagen, S., and Sallam, M.A.E.: Synthetic and spectroscopic studies of 2-C-methyl-
956 erythritol and 2-C-methyl-threitol, *Phytochemistry*, 19, 2375-2377, 10.1016/s0031-9422(00)91030-6,
957 1980.
- 958 Barrett, T. E., Robinson, E. M., Usenko, S., and Sheesley, R. J.: Source Contributions to Wintertime
959 Elemental and Organic Carbon in the Western Arctic Based on Radiocarbon and Tracer Apportionment,
960 *Environmental Science & Technology*, 49, 11631-11639, 10.1021/acs.est.5b03081, 2015.
- 961 Barrett, T. E., and Sheesley, R. J.: Year-round optical properties and source characterization of Arctic
962 organic carbon aerosols on the North Slope Alaska, *Journal of Geophysical Research-Atmospheres*, 122,
963 9319-9331, 10.1002/2016jd026194, 2017.
- 964 Bates, K. H., Crouse, J. D., St Clair, J. M., Bennett, N. B., Nguyen, T. B., Seinfeld, J. H., Stoltz, B. M.,
965 and Wennberg, P. O.: Gas Phase Production and Loss of Isoprene Epoxydiols, *Journal of Physical*
966 *Chemistry A*, 118, 1237-1246, 10.1021/jp4107958, 2014.
- 967 Bauer, H., Kasper-Giebl, A., Loflund, M., Giebl, H., Hitzenberger, R., Zibuschka, F., and Puxbaum, H.:
968 The contribution of bacteria and fungal spores to the organic carbon content of cloud water, precipitation
969 and aerosols, *Atmospheric Research*, 64, 109-119, 10.1016/s0169-8095(02)00084-4, 2002.
- 970 Bond, T. C., Doherty, S. J., Fahey, D. W., Forster, P. M., Berntsen, T., DeAngelo, B. J., Flanner, M. G.,
971 Ghan, S., Karcher, B., Koch, D., Kinne, S., Kondo, Y., Quinn, P. K., Sarofim, M. C., Schultz, M. G.,
972 Schulz, M., Venkataraman, C., Zhang, H., Zhang, S., Bellouin, N., Guttikunda, S. K., Hopke, P. K.,
973 Jacobson, M. Z., Kaiser, J. W., Klimont, Z., Lohmann, U., Schwarz, J. P., Shindell, D., Storelvmo, T.,

- 974 Warren, S. G., and Zender, C. S.: Bounding the role of black carbon in the climate system: A scientific
975 assessment, *Journal of Geophysical Research-Atmospheres*, 118, 5380-5552, 10.1002/jgrd.50171, 2013.
- 976 Brighty, A., Jacob, V., Uzu, G., Borlaza, L., Conil, S., Hueglin, C., Grange, S. K., Favez, O., Trebuchon,
977 C., and Jaffrezo, J. L.: Cellulose in atmospheric particulate matter at rural and urban sites across France
978 and Switzerland, *Atmospheric Chemistry and Physics*, 22, 6021-6043, 10.5194/acp-22-6021-2022,
979 2022.
- 980 Cahill, T. M., Seaman, V. Y., Charles, M. J., Holzinger, R., and Goldstein, A. H.: Secondary organic
981 aerosols formed from oxidation of biogenic volatile organic compounds in the Sierra Nevada Mountains
982 of California, *Journal of Geophysical Research-Atmospheres*, 111, 10.1029/2006jd007178, 2006.
- 983 Cassiani, M., Stohl, A., and Brioude, J.: Lagrangian Stochastic Modelling of Dispersion in the
984 Convective Boundary Layer with Skewed Turbulence Conditions and a Vertical Density Gradient:
985 Formulation and Implementation in the FLEXPART Model, *Boundary-Layer Meteorology*, 154, 367-
986 390, 10.1007/s10546-014-9976-5, 2015.
- 987 Cavalli, F., Viana, M., Yttri, K. E., Genberg, J., and Putaud, J.-P.: Toward a standardised thermal-optical
988 protocol for measuring atmospheric organic and elemental carbon: the EUSAAR protocol, *Atmospheric
989 Measurement Techniques*, 3, 79-89, 2010.
- 990 Cavalli, F., Alastuey, A., Areskoug, H., Ceburnis, D., Cech, J., Genberg, J., Harrison, R. M., Jaffrezo,
991 J. L., Kiss, G., Laj, P., Mihalopoulos, N., Perez, N., Quincey, P., Schwarz, J., Sellegri, K., Spindler, G.,
992 Swietlicki, E., Theodosi, C., Yttri, K. E., Aas, W., and Putaud, J. P.: A European aerosol
993 phenomenology-4: Harmonized concentrations of carbonaceous aerosol at 10 regional background sites
994 across Europe, *Atmospheric Environment*, 144, 133-145, 10.1016/j.atmosenv.2012.07.050, 2016.
- 995 Claeys, M., Graham, B., Vas, G., Wang, W., Vermeylen, R., Pashynska, V., Cafmeyer, J., Guyon, P.,
996 Andreae, M. O., Artaxo, P., and Maenhaut, W.: Formation of secondary organic aerosols through
997 photooxidation of isoprene, *Science*, 303, 1173-1176, 10.1126/science.1092805, 2004.
- 998 Claeys, M., Kourtchev, I., Pashynska, V., Vas, G., Vermeylen, R., Wang, W., Cafmeyer, J., Chi, X.,
999 Artaxo, P., Andreae, M. O., and Maenhaut, W.: Polar organic marker compounds in atmospheric
1000 aerosols during the LBA-SMOCC 2002 biomass burning experiment in Rondonia, Brazil: sources and
1001 source processes, time series, diel variations and size distributions, *Atmospheric Chemistry and Physics*,
1002 10, 9319-9331, 10.5194/acp-10-9319-2010, 2010.
- 1003 Clarke, A. D., and Noone, K. J.: Soot in the Arctic snowpack - A cause for perturbations in radiative-
1004 transfer, *Atmospheric Environment*, 19, 2045-2053, 10.1016/0004-6981(85)90113-1, 1985.
- 1005 Coen, M. C., Andrews, E., Alastuey, A., Arsov, T. P., Backman, J., Brem, B. T., Bukowiecki, N., Couret,
1006 C., Eleftheriadis, K., Flentje, H., Fiebig, M., Gysel-Beer, M., Hand, J. L., Hoffer, A., Hooda, R.,
1007 Hueglin, C., Joubert, W., Keywood, M., Kim, J. E., Kim, S. W., Labuschagne, C., Lin, N. H., Lin, Y.,
1008 Myhre, C. L., Luoma, K., Lyamani, H., Marinoni, A., Mayol-Bracero, O. L., Mihalopoulos, N., Pandolfi,
1009 M., Prats, N., Prenni, A. J., Putaud, J. P., Ries, L., Reisen, F., Sellegri, K., Sharma, S., Sheridan, P.,
1010 Sherman, J. P., Sun, J. Y., Titos, G., Torres, E., Tuch, T., Weller, R., Wiedensohler, A., Zieger, P., and
1011 Laj, P.: Multidecadal trend analysis of in situ aerosol radiative properties around the world, *Atmospheric
1012 Chemistry and Physics*, 20, 8867-8908, 10.5194/acp-20-8867-2020, 2020.
- 1013 Creamean, J. M., Kirpes, R. M., Pratt, K. A., Spada, N. J., Maahn, M., de Boer, G., Schnell, R. C., and
1014 China, S.: Marine and terrestrial influences on ice nucleating particles during continuous springtime
1015 measurements in an Arctic oilfield location, *Atmospheric Chemistry and Physics*, 18, 18023-18042,
1016 10.5194/acp-18-18023-2018, 2018.

- 1017 Creamean, J. M., Mignani, C., Bukowiecki, N., and Conen, F.: Using freezing spectra characteristics to
1018 identify ice-nucleating particle populations during the winter in the Alps, *Atmospheric Chemistry and*
1019 *Physics*, 19, 8123-8140, 10.5194/acp-19-8123-2019, 2019.
- 1020 Creamean, J. M., Hill, T. C. J., DeMott, P. J., Uetake, J., Kreidenweis, S., and Douglas, T. A.: Thawing
1021 permafrost: an overlooked source of seeds for Arctic cloud formation, *Environmental Research Letters*,
1022 15, 10.1088/1748-9326/ab87d3, 2020.
- 1023 Creamean, J. M., Barry, K., Hill, T. C., Hume, C., DeMott, P. J., Shupe, M. D., Dahlke, S., Willmes, S.,
1024 Schmale, J., Beck, I., Hoppe, C. J. M., Fong, A., Chamberlain, E., Bowman, J., Scharien, R., and
1025 Persson, O.: Annual cycle observations of aerosols capable of ice formation in central Arctic clouds,
1026 *Nat. Commun.*, 13, 1–12, 2022.
- 1027 Cui, T. Q., Zeng, Z. X., dos Santos, E. O., Zhang, Z. F., Chen, Y. Z., Zhang, Y., Rose, C. A.,
1028 Budisulistiorini, S. H., Collins, L. B., Bodnar, W. M., de Souza, R. A. F., Martin, S. T., Machado, C. M.
1029 D., Turpin, B. J., Gold, A., Ault, A. P., and Surratt, J. D.: Development of a hydrophilic interaction
1030 liquid chromatography (HILIC) method for the chemical characterization of water-soluble isoprene
1031 epoxydiol (IEPOX)-derived secondary organic aerosol, *Environmental Science-Processes & Impacts*,
1032 20, 1524-1536, 10.1039/c8em00308d, 2018.
- 1033 Dani, K. G. S., and Loreto, F.: Trade-Off Between Dimethyl Sulfide and Isoprene Emissions from
1034 Marine Phytoplankton, *Trends in Plant Science*, 22, 361-372, 10.1016/j.tplants.2017.01.006, 2017.
- 1035 Darer, A. I., Cole-Filipiak, N. C., O'Connor, A. E., Elrod, M. J.: Formation and Stability of
1036 Atmospherically Relevant Isoprene-Derived Organosulfates and Organonitrates, *Environ. Sci. Technol.*
1037 45 (5), 1895 – 1902, <https://doi.org/10.1021/es103797z>, 2011.
- 1038 Dittrich, P., and Angyal, S. J.: 2-C-methyl-erythritol in leaves of *Liriodendron-tulipifera*,
1039 *Phytochemistry*, 27, 935-935, 10.1016/0031-9422(88)84125-6, 1988.
- 1040 Duvold, T., Bravo, J. M., PaleGrosdemange, C., and Rohmer, M.: Biosynthesis of 2-C-methyl-D-
1041 erythritol, a putative C-5 intermediate in the mevalonate independent pathway for isoprenoid
1042 biosynthesis, *Tetrahedron Letters*, 38, 4769-4772, 10.1016/s0040-4039(97)01045-9, 1997.
- 1043 Dye, C., and Yttri, K.: Determination of monosaccharide anhydrides in atmospheric aerosols by use of
1044 high-performance liquid chromatography combined with high-resolution mass spectrometry, *Analytical*
1045 *Chemistry*, 77, 1853-1858, 10.1021/ac049461j, 2005.
- 1046 Elbert, W., Taylor, P. E., Andreae, M. O., and Poschl, U.: Contribution of fungi to primary biogenic
1047 aerosols in the atmosphere: wet and dry discharged spores, carbohydrates, and inorganic ions,
1048 *Atmospheric Chemistry and Physics*, 7, 4569-4588, 10.5194/acp-7-4569-2007, 2007.
- 1049 El Haddad, I., Marchand, N., Temime-Roussel, B., Wortham, H., Piot, C., Besombes, J. L., Baduel, C.,
1050 Voisin, D., Armengaud, A., and Jaffrezo, J. L.: Insights into the secondary fraction of the organic aerosol
1051 in a Mediterranean urban area: Marseille, *Atmospheric Chemistry and Physics*, 11, 2059-2079,
1052 10.5194/acp-11-2059-2011, 2011.
- 1053 Eleftheriadis, K., Vratolis, S., and Nyeki, S.: Aerosol black carbon in the European Arctic:
1054 Measurements at Zeppelin station, Ny-Alesund, Svalbard from 1998-2007, *Geophysical Research*
1055 *Letters*, 36, 10.1029/2008gl035741, 2009.
- 1056 Enomoto, H., Kohata, K., Nakayama, M., Yamaguchi, Y., and Ichimura, K.: 2-C-methyl-D-erythritol is
1057 a major carbohydrate in petals of *Phlox subulata* possibly involved in flower development, *Journal of*
1058 *Plant Physiology*, 161, 977-980, 10.1016/j.jplph.2004.01.009, 2004.

- 1059 EU Action on Black Carbon in the Arctic: Review of Observation Capacities and Data Availability for
 1060 Black Carbon in the Arctic Region: EU Action on Black Carbon in the Arctic – Technical Report 1. 35
 1061 pp. <https://www.amap.no/work-area/document/3058>, 2019
- 1062 Feltracco, M., Barbaro, E., Tedeschi, S., Spolaor, A., Turetta, C., Vecchiato, M., Morabito, E.,
 1063 Zangrando, R., Barbante, C., and Gambaro, A.: Interannual variability of sugars in Arctic aerosol:
 1064 Biomass burning and biogenic inputs, *Science of the Total Environment*, 706,
 1065 10.1016/j.scitotenv.2019.136089, 2020.
- 1066 Ferrero, L., Sangiorgi, G., Perrone, M. G., Rizzi, C., Cataldi, M., Markuszewski, P., Pakszys, P.,
 1067 Makuch, P., Petelski, T., Becagli, S., Traversi, R., Bolzacchini, E., and Zielinski, T.: Chemical
 1068 Composition of Aerosol over the Arctic Ocean from Summer ARctic EXpedition (AREX) 2011-2012
 1069 Cruises: Ions, Amines, Elemental Carbon, Organic Matter, Polycyclic Aromatic Hydrocarbons, n-
 1070 Alkanes, Metals, and Rare Earth Elements, *Atmosphere*, 10, 10.3390/atmos10020054, 2019.
- 1071 Forster, C., Stohl, A., and Seibert, P.: Parameterization of convective transport in a Lagrangian particle
 1072 dispersion model and its evaluation, *Journal of Applied Meteorology and Climatology*, 46, 403-422,
 1073 10.1175/jam2470.1, 2007.
- 1074 Freitas, G.P., Adachi, K., Conen, F., Heslin-Rees, D., Krejci, R., Tobo, Y., Yttri, K.E. and Zieger, P.
 1075 Regionally sourced bioaerosols drive high-temperature ice nucleating particles in the Arctic. *Nat*
 1076 *Commun* 14, 5997 (2023). <https://doi.org/10.1038/s41467-023-41696-7>
- 1077 Fu, P. Q., Kawamura, K., Chen, J., and Barrie, L. A.: Isoprene, Monoterpene, and Sesquiterpene
 1078 Oxidation Products in the High Arctic Aerosols during Late Winter to Early Summer, *Environmental*
 1079 *Science & Technology*, 43, 4022-4028, 10.1021/es803669a, 2009a.
- 1080 Fu, P. Q., Kawamura, K., and Barrie, L. A.: Photochemical and Other Sources of Organic Compounds
 1081 in the Canadian High Arctic Aerosol Pollution during Winter-Spring, *Environmental Science &*
 1082 *Technology*, 43, 286-292, 10.1021/es803046q, 2009b.
- 1083 Fu, P. Q., Kawamura, K., Kanaya, Y., and Wang, Z. F.: Contributions of biogenic volatile organic
 1084 compounds to the formation of secondary organic aerosols over Mt Tai, Central East China,
 1085 *Atmospheric Environment*, 44, 4817-4826, 10.1016/j.atmosenv.2010.08.040, 2010.
- 1086 Fu, P. Q., Kawamura, K., Chen, J., Charriere, B., and Sempere, R.: Organic molecular composition of
 1087 marine aerosols over the Arctic Ocean in summer: contributions of primary emission and secondary
 1088 aerosol formation, *Biogeosciences*, 10, 653-667, 10.5194/bg-10-653-2013, 2013.
- 1089 Garg, S., Chandra, B. P., Sinha, V., Sarda-Estevé, R., Gros, V., and Sinha, B.: Limitation of the Use of
 1090 the Absorption Angstrom Exponent for Source Apportionment of Equivalent Black Carbon: a Case
 1091 Study from the North West Indo-Gangetic Plain, *Environmental Science & Technology*, 50, 814-824,
 1092 10.1021/acs.est.5b03868, 2016
- 1093 Gelencser, A., May, B., Simpson, D., Sanchez-Ochoa, A., Kasper-Giebl, A., Puxbaum, H., Caseiro, A.,
 1094 Pio, C., and Legrand, M.: Source apportionment of PM_{2.5} organic aerosol over Europe:
 1095 Primary/secondary, natural/anthropogenic, and fossil/biogenic origin, *Journal of Geophysical Research-*
 1096 *Atmospheres*, 112, 10.1029/2006jd008094, 2007.
- 1097 Genberg, J., Hyder, M., Stenstrom, K., Bergstrom, R., Simpson, D., Fors, E. O., Jonsson, J. A., and
 1098 Swietlicki, E.: Source apportionment of carbonaceous aerosol in southern Sweden, *Atmospheric*
 1099 *Chemistry and Physics*, 11, 11387-11400, 10.5194/acp-11-11387-2011, 2011.

- 1100 Giglio, L., Descloitres, J., Justice, C. O., and Kaufman, Y. J.: An enhanced contextual fire detection
1101 algorithm for MODIS, *Remote Sensing of Environment*, 87, 273-282, 10.1016/s0034-4257(03)00184-
1102 6, 2003.
- 1103 Gilardoni, S., Vignati, E., Cavalli, F., Putaud, J. P., Larsen, B. R., Karl, M., Stenstrom, K., Genberg, J.,
1104 Henne, S., and Dentener, F.: Better constraints on sources of carbonaceous aerosols using a combined
1105 C-14 - macro tracer analysis in a European rural background site, *Atmospheric Chemistry and Physics*,
1106 11, 5685-5700, 10.5194/acp-11-5685-2011, 2011.
- 1107 Glasius, M., Hansen, A. M. K., Claeys, M., Henzing, J. S., Jedynska, A. D., Kasper-Giebl, A., Kistler,
1108 M., Kristensen, K., Martinsson, J., Maenhaut, W., Nojgaard, J. K., Spindler, G., Stenstrom, K. E.,
1109 Swietlicki, E., Szidat, S., Simpson, D., and Yttri, K. E.: Composition and sources of carbonaceous
1110 aerosols in Northern Europe during winter, *Atmospheric Environment*, 173, 127-141,
1111 10.1016/j.atmosenv.2017.11.005, 2018.
- 1112 Gonzalez, N. J. D., Borg-Karlson, A. K., Artaxo, P., Guenther, A., Krejci, R., Noziere, B., and Noone,
1113 K.: Primary and secondary organics in the tropical Amazonian rainforest aerosols: chiral analysis of 2-
1114 methyltetraols, *Environmental Science-Processes & Impacts*, 16, 1413-1421, 10.1039/c4em00102h,
1115 2014.
- 1116 Graham, B., Guyon, P., Taylor, P. E., Artaxo, P., Maenhaut, W., Glovsky, M. M., Flagan, R.C., and
1117 Andreae, M. O.: Organic compounds present in the natural Amazonian aerosol: Character- ization by
1118 gas chromatography-mass spectrometry, *J. Geophys. Res.*, 108, 4766, doi:10.1029/2003JD003990,
1119 2003.
- 1120 Grythe, H., Kristiansen, N. I., Zwaafink, C. D. G., Eckhardt, S., Strom, J., Tunved, P., Krejci, R., and
1121 Stohl, A.: A new aerosol wet removal scheme for the Lagrangian particle model FLEXPART v10,
1122 *Geoscientific Model Development*, 10, 1447-1466, 10.5194/gmd-10-1447-2017, 2017.
- 1123 Hallquist, M., Wenger, J. C., Baltensperger, U., Rudich, Y., Simpson, D., Claeys, M., Dommen, J.,
1124 Donahue, N. M., George, C., Goldstein, A. H., Hamilton, J. F., Herrmann, H., Hoffmann, T., Iinuma,
1125 Y., Jang, M., Jenkin, M. E., Jimenez, J. L., Kiendler-Scharr, A., Maenhaut, W., McFiggans, G., Mentel,
1126 T. F., Monod, A., Prevot, A. S. H., Seinfeld, J. H., Surratt, J. D., Szmigielski, R., and Wildt, J.: The
1127 formation, properties and impact of secondary organic aerosol: current and emerging issues,
1128 *Atmospheric Chemistry and Physics*, 9, 5155-5236, 10.5194/acp-9-5155-2009, 2009.
- 1129 Hansen, A. M. K., Kristensen, K., Nguyen, Q. T., Zare, A., Cozzi, F., Nojgaard, J. K., Skov, H., Brandt,
1130 J., Christensen, J. H., Strom, J., Tunved, P., Krejci, R., and Glasius, M.: Organosulfates and organic
1131 acids in Arctic aerosols: speciation, annual variation and concentration levels, *Atmospheric Chemistry
1132 and Physics*, 14, 7807-7823, 10.5194/acp-14-7807-2014, 2014.
- 1133 Hansen, J., and Nazarenko, L.: Soot climate forcing via snow and ice albedos, *Proceedings of the
1134 National Academy of Sciences of the United States of America*, 101, 423-428,
1135 10.1073/pnas.2237157100, 2004.
- 1136 Hartmann, M., Blunier, T., Brugger, S. O., Schmale, J., Schwikowski, M., Vogel, A., Wex, H., and
1137 Stratmann, F.: Variation of Ice Nucleating Particles in the European Arctic Over the Last Centuries,
1138 *Geophysical Research Letters*, 46, 4007-4016, 10.1029/2019gl082311, 2019.
- 1139 Hartmann, M., Adachi, K., Eppers, O., Haas, C., Herber, A., Holzinger, R., Hunerbein, A., Jakel, E.,
1140 Jentsch, C., van Pinxteren, M., Wex, H., Willmes, S., and Stratmann, F.: Wintertime Airborne
1141 Measurements of Ice Nucleating Particles in the High Arctic: A Hint to a Marine, Biogenic Source for
1142 Ice Nucleating Particles, *Geophysical Research Letters*, 47, 10.1029/2020gl087770, 2020.

- 1143 Hersbach, H., Bell, B., Berrisford, P., Hirahara, S., Horanyi, A., Muñoz-Sabater, J., Nicolas, J., Peubey,
 1144 C., Radu, R., Schepers, D., Simmons, A., Soci, C., Abdalla, S., Abellan, X., Balsamo, G., Bechtold, P.,
 1145 Biavati, G., Bidlot, J., Bonavita, M., De Chiara, G., Dahlgren, P., Dee, D., Diamantakis, M., Dragani,
 1146 R., Flemming, J., Forbes, R., Fuentes, M., Geer, A., Haimberger, L., Healy, S., Hogan, R. J., Holm, E.,
 1147 Janiskova, M., Keeley, S., Laloyaux, P., Lopez, P., Lupu, C., Radnoti, G., de Rosnay, P., Rozum, I.,
 1148 Vamborg, F., Villaume, S., and Thepaut, J. N.: The ERA5 global reanalysis, *Quarterly Journal of the*
 1149 *Royal Meteorological Society*, 146, 1999-2049, 10.1002/qj.3803, 2020.
- 1150 Heslin-Rees, D., Burgos, M., Hansson, H. C., Krejci, R., Strom, J., Tunved, P., and Zieger, P.: From a
 1151 polar to a marine environment: has the changing Arctic led to a shift in aerosol light scattering
 1152 properties?, *Atmospheric Chemistry and Physics*, 20, 13671-13686, 10.5194/acp-20-13671-2020, 2020.
- 1153 Hirdman, D., Sodemann, H., Eckhardt, S., Burkhardt, J. F., Jefferson, A., Mefford, T., Quinn, P. K.,
 1154 Sharma, S., Strom, J., and Stohl, A.: Source identification of short-lived air pollutants in the Arctic using
 1155 statistical analysis of measurement data and particle dispersion model output, *Atmospheric Chemistry*
 1156 *and Physics*, 10, 669-693, 10.5194/acp-10-669-2010, 2010.
- 1157 Hodshire, A. L., Campuzano-Jost, P., Kodros, J. K., Croft, B., Nault, B. A., Schroder, J. C., Jimenez, J.
 1158 L., and Pierce, J. R.: The potential role of methanesulfonic acid (MSA) in aerosol formation and growth
 1159 and the associated radiative forcings, *Atmospheric Chemistry and Physics*, 19, 3137-3160, 10.5194/acp-
 1160 19-3137-2019, 2019.
- 1161 Horn, S. J., Aasen, I. M., and Ostgaard, K.: Ethanol production from seaweed extract, *Journal of*
 1162 *Industrial Microbiology & Biotechnology*, 25, 249-254, 10.1038/sj.jim.7000065, 2000.
- 1163 Hu, Q. H., Xie, Z. Q., Wang, X. M., Kang, H., and Zhang, P. F.: Levoglucosan indicates high levels of
 1164 biomass burning aerosols over oceans from the Arctic to Antarctic, *Scientific Reports*, 3, 7,
 1165 10.1038/srep03119, 2013.
- 1166 Ion, A. C., Vermeylen, R., Kourtchev, I., Cafmeyer, J., Chi, X., Gelencser, A., Maenhaut, W., and
 1167 Claeys, M.: Polar organic compounds in rural PM_{2.5} aerosols from K-pusztá, Hungary, during a 2003
 1168 summer field campaign: Sources and diel variations, *Atmospheric Chemistry and Physics*, 5, 1805-1814,
 1169 10.5194/acp-5-1805-2005, 2005.
- 1170 Jacobsen, E. E., and Anthonsen, T.: 2-C-Methyl-D-erythritol. Produced in plants, forms aerosols in the
 1171 atmosphere. An alternative pathway in isoprenoid biosynthesis, *Biocatalysis and Biotransformation*, 33,
 1172 191-196, 10.3109/10242422.2015.1095677, 2015.
- 1173 Jiao, C. Y., and Flanner, M. G.: Changing black carbon transport to the Arctic from present day to the
 1174 end of 21st century, *Journal of Geophysical Research-Atmospheres*, 121, 4734-4750,
 1175 10.1002/2015jd023964, 2016.
- 1176 Jurányi, Z., Zanatta, M., Lund, M.T., Samset, B.H., Skeie, R.B., Sharma, S., Wendisch, M., Herber, A.:
 1177 Atmospheric concentrations of black carbon are substantially higher in spring than summer in the Arctic.
 1178 *Communications Earth & Environment* 4, 91, 2023. <https://doi.org/10.1038/s43247-023-00749-x>.
- 1179 Karlsen, S. R., Elvebakk, A., Hogda, K. A., and Grydeland, T.: Spatial and Temporal Variability in the
 1180 Onset of the Growing Season on Svalbard, Arctic Norway - Measured by MODIS-NDVI Satellite Data,
 1181 *Remote Sensing*, 6, 8088-8106, 10.3390/rs6098088, 2014.
- 1182 Klimont, Z., Kupiainen, K., Heyes, C., Purohit, P., Cofala, J., Rafaj, P., Borcken-Kleefeld, J., and Schopp,
 1183 W.: Global anthropogenic emissions of particulate matter including black carbon, *Atmospheric*
 1184 *Chemistry and Physics*, 17, 8681-8723, 10.5194/acp-17-8681-2017, 2017.

- 1185 Kourtchev, I., Ruuskanen, T., Maenhaut, W., Kulmala, M., and Claeys, M.: Observation of 2-
1186 methyltetrols and related photo-oxidation products of isoprene in boreal forest aerosols from Hyytiala,
1187 Finland, *Atmospheric Chemistry and Physics*, 5, 2761-2770, 10.5194/acp-5-2761-2005, 2005.
- 1188 Kourtchev, I., Ruuskanen, T. M., Keronen, P., Sogacheva, L., Dal Maso, M., Reissell, A., Chi, X.,
1189 Vermeylen, R., Kulmala, M., Maenhaut, W., and Claeys, M.: Determination of isoprene and alpha-/beta-
1190 pinene oxidation products in boreal forest aerosols from Hyytiala, Finland: diel variations and possible
1191 link with particle formation events, *Plant Biology*, 10, 138-149, 10.1055/s-2007-964945, 2008a.
- 1192 Kourtchev, I., Warnke, J., Maenhaut, W., Hoffmann, T., and Claeys, M.: Polar organic marker
1193 compounds in PM_{2.5} aerosol from a mixed forest site in western Germany, *Chemosphere*, 73, 1308-
1194 1314, 10.1016/j.chemosphere.2008.07.011, 2008b.
- 1195 Kramshoj, M., Vedel-Petersen, I., Schollert, M., Rinnan, A., Nymand, J., Ro-Poulsen, H., and Rinnan,
1196 R.: Large increases in Arctic biogenic volatile emissions are a direct effect of warming, *Nature*
1197 *Geoscience*, 9, 349-+, 10.1038/ngeo2692, 2016.
- 1198 Kunit, M., and Puxbaum, H.: Enzymatic determination of the cellulose content of atmospheric aerosols,
1199 *Atmospheric Environment*, 30, 1233-1236, 10.1016/1352-2310(95)00429-7, 1996.
- 1200 Li, S. M., Barrie, L. A., and Sirois, A.: Biogenic sulfur aerosol in the Arctic troposphere. 2. Trends and
1201 seasonal-variations, *Journal of Geophysical Research-Atmospheres*, 98, 20623-20631,
1202 10.1029/93jd02233, 1993.
- 1203 Liakakou, E., Vrekoussis, M., Bonsang, B., Donousis, C., Kanakidou, M., and Mihalopoulos, N.:
1204 Isoprene above the Eastern Mediterranean: Seasonal variation and contribution to the oxidation capacity
1205 of the atmosphere, *Atmospheric Environment*, 41, 1002-1010, 10.1016/j.atmosenv.2006.09.034, 2007.
- 1206 Lin, Y. H., Zhang, Z. F., Docherty, K. S., Zhang, H. F., Budisulistiorini, S. H., Rubitschun, C. L.,
1207 Shaw, S. L., Knipping, E. M., Edgerton, E. S., Kleindienst, T. E., Gold, A., and Surratt, J. D.: Isoprene
1208 Epoxydiols as Precursors to Secondary Organic Aerosol Formation: Acid-Catalyzed Reactive Uptake
1209 Studies with Authentic Compounds, *Environmental Science & Technology*, 46, 250-258,
1210 10.1021/es202554c, 2012.
- 1211 Long, C. M., Nascarella, M. A., and Valberg, P. A.: Carbon black vs. black carbon and other airborne
1212 materials containing elemental carbon: Physical and chemical distinctions, *Environmental Pollution*,
1213 181, 271-286, 10.1016/j.envpol.2013.06.009, 2013.
- 1214 Lopez-Hilfiker, F. D., Mohr, C., D'Ambro, E. L., Lutz, A., Riedel, T. P., Gaston, C. J., Iyer, S., Zhang,
1215 Z., Gold, A., Surratt, J. D., Lee, B. H., Kurten, T., Hu, W. W., Jimenez, J., Hallquist, M., and Thornton,
1216 J. A.: Molecular Composition and Volatility of Organic Aerosol in the Southeastern US: Implications
1217 for IEPDX Derived SOA, *Environmental Science & Technology*, 50, 2200-2209,
1218 10.1021/acs.est.5b04769, 2016.
- 1219 McCarty, J. L., Aalto, J., Paunu, V. V., Arnold, S. R., Eckhardt, S., Klimont, Z., Fain, J. J., Evangelidou,
1220 N., Venalainen, A., Tchepakova, N. M., Parfenova, E. I., Kupiainen, K., Soja, A. J., Huang, L., and
1221 Wilson, S.: Reviews and syntheses: Arctic fire regimes and emissions in the 21st century,
1222 *Biogeosciences*, 18, 5053-5083, 10.5194/bg-18-5053-2021, 2021.
- 1223 McDow, S. R., and Huntzicker, J. J.: Organic Aerosol Sampling Artifacts, *Abstracts of Papers of the*
1224 *American Chemical Society*, 200, 106-Envr, 1990.

- 1225 Medeiros, P. M., Conte, M. H., Weber, J. C., and Simoneit, B. R. T.: Sugars as source indicators of
 1226 biogenic organic carbon in aerosols collected above the Howland Experimental Forest, Maine,
 1227 *Atmospheric Environment*, 40, 1694-1705, 10.1016/j.atmosenv.2005.11.001, 2006.
- 1228 Moschos, V., Dzepina, K., Bhattu, D., Lamkaddam, H., Casotto, R., Daellenbach, K. R., Canonaco, F.,
 1229 Rai, P., Aas, W., Becagli, S., Calzolari, G., Eleftheriadis, K., Moffett, C. E., Schnelle-Kreis, J., Severi,
 1230 M., Sharma, S., Skov, H., Vestenius, M., Zhang, W., Hakola, H., Hellén, H., Huang, L., Jaffrezo, J.-L.,
 1231 Massling, A., Nøjgaard, J. K., Petäjä, T., Popovicheva, O., Sheesley, R. J., Traversi, R., Yttri, K. E.,
 1232 Schmale, J., Prévôt, A. S. H., Baltensperger, U., and El Haddad, I.: Equal abundance of summertime
 1233 natural and wintertime anthropogenic Arctic organic aerosols, *Nature Geoscience*, 10.1038/s41561-021-
 1234 00891-1, 2022.
- 1235 Myers-Smith, I. H., Kerby, J. T., Phoenix, G. K., Bjerke, J. W., Epstein, H. E., Assmann, J. J., John, C.,
 1236 Andreu-Hayles, L., Angers-Blondin, S., Beck, P. S. A., Berner, L. T., Bhatt, U. S., Bjorkman, A. D.,
 1237 Blok, D., Bryn, A., Christiansen, C. T., Cornelissen, J. H. C., Cunliffe, A. M., Elmendorf, S. C., Forbes,
 1238 B. C., Goetz, S. J., Hollister, R. D., de Jong, R., Loranty, M. M., Macias-Fauria, M., Maseyk, K.,
 1239 Normand, S., Olofsson, J., Parker, T. C., Parmentier, F. J. W., Post, E., Schaepman-Strub, G., Stordal,
 1240 F., Sullivan, P. F., Thomas, H. J. D., Tommervik, H., Treharne, R., Tweedie, C. E., Walker, D. A.,
 1241 Wilmking, M., and Wipf, S.: Complexity revealed in the greening of the Arctic, *Nature Climate Change*,
 1242 10, 106-117, 10.1038/s41558-019-0688-1, 2020.
- 1243 Nolte, C. G., Schauer, J. J., Cass, G. R., and Simoneit, B. R. T.: Highly polar organic compounds present
 1244 in wood smoke and in the ambient atmosphere, *Environmental Science & Technology*, 35, 1912-1919,
 1245 10.1021/es001420r, 2001.
- 1246 Noziere, B., Gonzalez, N. J. D., Borg-Karlson, A. K., Pei, Y. X., Redeby, J. P., Krejci, R., Dommen, J.,
 1247 Prevot, A. S. H., and Anthonsen, T.: Atmospheric chemistry in stereo: A new look at secondary organic
 1248 aerosols from isoprene, *Geophysical Research Letters*, 38, 10.1029/2011gl047323, 2011.
- 1249 Noziere, B., Kalberer, M., Claeys, M., Allan, J., D'Anna, B., Decesari, S., Finessi, E., Glasius, M., Grgic,
 1250 I., Hamilton, J. F., Hoffmann, T., Iinuma, Y., Jaoui, M., Kahno, A., Kampf, C. J., Kourtschev, I.,
 1251 Maenhaut, W., Marsden, N., Saarikoski, S., Schnelle-Kreis, J., Surratt, J. D., Szidat, S., Szmigielski, R.,
 1252 and Wisthaler, A.: The Molecular Identification of Organic Compounds in the Atmosphere: State of the
 1253 Art and Challenges, *Chemical Reviews*, 115, 3919-3983, 10.1021/cr5003485, 2015a.
- 1254 Ottar, B.: Arctic air-pollution - A Norwegian Perspective, *Atmospheric Environment*, 23, 2349-2356,
 1255 10.1016/0004-6981(89)90248-5, 1989.
- 1256 Paasonen, P., Asmi, A., Petaja, T., Kajos, M. K., Aijala, M., Junninen, H., Holst, T., Abbatt, J. P. D.,
 1257 Arneth, A., Birmili, W., van der Gon, H. D., Hamed, A., Hoffer, A., Laakso, L., Laaksonen, A., Leaitch,
- 1258 Paulot, F., Crouse, J. D., Kjaergaard, H. G., Kurten, A., St Clair, J. M., Seinfeld, J. H., and Wennberg,
 1259 P. O.: Unexpected Epoxide Formation in the Gas-Phase Photooxidation of Isoprene, *Science*, 325, 730-
 1260 733, 10.1126/science.1172910, 2009.
- 1261 Pisso, I., Sollum, E., Grythe, H., Kristiansen, N. I., Cassiani, M., Eckhardt, S., Arnold, D., Morton, D.,
 1262 Thompson, R. L., Zwaafink, C. D. G., Evangeliou, N., Sodemann, H., Haimberger, L., Henne, S.,
 1263 Brunner, D., Burkhardt, J. F., Fouilloux, A., Brioude, J., Philipp, A., Seibert, P., and Stohl, A.: The
 1264 Lagrangian particle dispersion model FLEXPART version 10.4, *Geoscientific Model Development*, 12,
 1265 4955-4997, 10.5194/gmd-12-4955-2019, 2019.
- 1266 Platt, S. M., Hov, O., Berg, T., Breivik, K., Eckhardt, S., Eleftheriadis, K., Evangeliou, N., Fiebig, M.,
 1267 Fisher, R., Hansen, G., Hansson, H. C., Heintzenberg, J., Hermansen, O., Heslin-Rees, D., Holmen, K.,
 1268 Hudson, S., Kallenborn, R., Krejci, R., Krognes, T., Larssen, S., Lowry, D., Myhre, C. L., Lunder, C.,

- 1269 Nisbet, E., Nizzetto, P. B., Park, K. T., Pedersen, C. A., Pfaffhuber, K. A., Rockmann, T., Schmidbauer,
1270 N., Solberg, S., Stohl, A., Strom, J., Svendby, T., Tunved, P., Tornkvist, K., van der Veen, C., Vratolis,
1271 S., Yoon, Y. J., Yttri, K. E., Zieger, P., Aas, W., and Torseth, K.: Atmospheric composition in the
1272 European Arctic and 30 years of the Zeppelin Observatory, Ny-Ålesund, *Atmospheric Chemistry and
1273 Physics*, 22, 3321-3369, 10.5194/acp-22-3321-2022, 2022.
- 1274 Platt, S. M., et al.: Source apportionment of equivalent black carbon from the winter 2017–2018 EMEP
1275 intensive measurement campaign using PMF, in preparation, 2023.
- 1276 Prospero, J. M., Blades, E., Mathison, G., and Naidu, R.: Interhemispheric transport of viable fungi and
1277 bacteria from Africa to the Caribbean with soil dust, *Aerobiologia*, 21, 1-19, 10.1007/s10453-004-5872-
1278 7, 2005.
- 1279 Pueschel, R. F., and Kinne, S. A.: Physical and radiative properties of Arctic atmospheric aerosols,
1280 *Science of the Total Environment*, 160-61, 811-824, 10.1016/0048-9697(95)04414-v, 1995.
- 1281 Puxbaum, H., and Tenze-Kunit, M.: Size distribution and seasonal variation of atmospheric cellulose,
1282 *Atmospheric Environment*, 37, 3693-3699, 10.1016/s1352-2310(03)00451-5, 2003.
- 1283 Qi, L., Vogel, A. L., Esmaeilrad, S., Cao, L. M., Zheng, J., Jaffrezo, J. L., Fermo, P., Kasper-Giebl, A.,
1284 Daellenbach, K. R., Chen, M. D., Ge, X. L., Baltensperger, U., Prevot, A. S. H., and Slowik, J. G.: A 1-
1285 year characterization of organic aerosol composition and sources using an extractive electrospray
1286 ionization time-of-flight mass spectrometer (EESI-TOF), *Atmospheric Chemistry and Physics*, 20,
1287 7875-7893, 10.5194/acp-20-7875-2020, 2020.
- 1288 Quinn, P. K., Miller, T. L., Bates, T. S., Ogren, J. A., Andrews, E., and Shaw, G. E.: A 3-year record of
1289 simultaneously measured aerosol chemical and optical properties at Barrow, Alaska, *Journal of
1290 Geophysical Research-Atmospheres*, 107, 10.1029/2001jd001248, 2002.
- 1291 Quinn, P. K., Shaw, G., Andrews, E., Dutton, E. G., Ruoho-Airola, T., and Gong, S. L.: Arctic haze:
1292 current trends and knowledge gaps, *Tellus Series B-Chemical and Physical Meteorology*, 59, 99-114,
1293 10.1111/j.1600-0889.2006.00238.x, 2007.
- 1294 Quinn, P. K., Bates, T. S., Schulz, K., and Shaw, G. E.: Decadal trends in aerosol chemical composition
1295 at Barrow, Alaska: 1976-2008, *Atmospheric Chemistry and Physics*, 9, 8883-8888, 10.5194/acp-9-
1296 8883-2009, 2009.
- 1297 Rauber, M., Salazar, G., Yttri, K. E., and Szidat, S.: An optimised organic carbon/elemental carbon
1298 (OC/EC) fraction separation method for radiocarbon source apportionment applied to low-loaded
1299 Arctic aerosol filters, *Atmos. Meas. Tech.*, 16, 825–844, <https://doi.org/10.5194/amt-16-825-2023>,
1300 2023.
- 1301
1302 Rauber, M. et al.: Organic aerosols at Trollhaugen Observatory (Antarctica) in summer are dominated
1303 by marine sources. In preparation, 2023.
- 1304 Ricard, V., Jaffrezo, J. L., Kerminen, V. M., Hillamo, R. E., Sillanpaa, M., Ruellan, S., Liousse, C., and
1305 Cachier, H.: Two years of continuous aerosol measurements in northern Finland, *Journal of Geophysical
1306 Research-Atmospheres*, 107, 10.1029/2001jd000952, 2002.
- 1307 Riipinen, I., Pierce, J. R., Yli-Juuti, T., Nieminen, T., Hakkinen, S., Ehn, M., Junninen, H., Lehtipalo,
1308 K., Petaja, T., Slowik, J., Chang, R., Shantz, N. C., Abbatt, J., Leaitch, W. R., Kerminen, V. M.,
1309 Worsnop, D. R., Pandis, S. N., Donahue, N. M., and Kulmala, M.: Organic condensation: a vital link
1310 connecting aerosol formation to cloud condensation nuclei (CCN) concentrations, *Atmospheric
1311 Chemistry and Physics*, 11, 3865-3878, 10.5194/acp-11-3865-2011, 2011.

- 1312 Rotzer, T., and Chmielewski, F. M.: Phenological maps of Europe, *Climate Research*, 18, 249-257,
1313 10.3354/cr018249, 2001.
- 1314 Sagner, S., Eisenreich, W., Fellermeier, M., Latzel, C., Bacher, A., and Zenk, M. H.: Biosynthesis of 2-
1315 C-methyl-D-erythritol in plants by rearrangement of the terpenoid precursor, 1-deoxy-D-xylulose 5-
1316 phosphate, *Tetrahedron Letters*, 39, 2091-2094, 10.1016/s0040-4039(98)00296-2, 1998.
- 1317 Samake, A., Jaffrezo, J. L., Favez, O., Weber, S., Jacob, V., Canete, T., Albinet, A., Charron, A.,
1318 Riffault, V., Perdrix, E., Waked, A., Golly, B., Salameh, D., Chevrier, F., Oliveira, D. M., Besombes, J.
1319 L., Martins, J. M. F., Bonnaire, N., Conil, S., Guillaud, G., Mesbah, B., Rocq, B., Robic, P. Y., Hulin,
1320 A., Le Meur, S., Descheemaeker, M., Chretien, E., Marchand, N., and Uzu, G.: Arabitol, mannitol, and
1321 glucose as tracers of primary biogenic organic aerosol: the influence of environmental factors on
1322 ambient air concentrations and spatial distribution over France, *Atmospheric Chemistry and Physics*,
1323 19, 11013-11030, 10.5194/acp-19-11013-2019, 2019.
- 1324 Samake, A., Bonin, A., Jaffrezo, J. L., Taberlet, P., Weber, S., Uzu, G., Jacob, V., Conil, S., and Martins,
1325 J. M. F.: High levels of primary biogenic organic aerosols are driven by only a few plant-associated
1326 microbial taxa, *Atmospheric Chemistry and Physics*, 20, 5609-5628, 10.5194/acp-20-5609-2020, 2020.
- 1327 Sanchez-Ochoa, A., Kasper-Giebl, A., Puxbaum, H., Gelencser, A., Legrand, M., and Pio, C.:
1328 Concentration of atmospheric cellulose: A proxy for plant debris across a west-east transect over Europe,
1329 *Journal of Geophysical Research-Atmospheres*, 112, 10.1029/2006jd008180, 2007.
- 1330 Sandradewi, J., Prevot, A. S. H., Szidat, S., Perron, N., Alfara, M. R., Lanz, V. A., Weingartner, E.,
1331 and Baltensperger, U.: Using aerosol light absorption measurements for the quantitative determination
1332 of wood burning and traffic emission contributions to particulate matter, *Environmental Science &
1333 Technology*, 42, 3316-3323, 10.1021/es702253m, 2008.
- 1334 Schmale, J., Zieger, P., and Ekman, A. M. L.: Aerosols in current and future Arctic climate, *Nature
1335 Climate Change*, 11, 95-105, 10.1038/s41558-020-00969-5, 2021.
- 1336 Schmidl, C., Marr, L. L., Caseiro, A., Kotianova, P., Berner, A., Bauer, H., Kasper-Giebl, A., and
1337 Puxbaum, H.: Chemical characterisation of fine particle emissions from wood stove combustion of
1338 common woods growing in mid-European Alpine regions, *Atmospheric Environment*, 42, 126-141,
1339 10.1016/j.atmosenv.2007.09.028, 2008.
- 1340 Serreze, M. C., and Barry, R. G.: Processes and impacts of Arctic amplification: A research synthesis,
1341 *Global and Planetary Change*, 77, 85-96, 10.1016/j.gloplacha.2011.03.004, 2011.
- 1342 Sharma, S., Chan, E., Ishizawa, M., Toom-Saunty, D., Gong, S. L., Li, S. M., Tarasick, D. W., Leaitch,
1343 W. R., Norman, A., Quinn, P. K., Bates, T. S., Lévassieur, M., Barrie, L. A., and Maenhaut, W.: Influence
1344 of transport and ocean ice extent on biogenic aerosol sulfur in the Arctic atmosphere, *Journal of
1345 Geophysical Research-Atmospheres*, 117, 10.1029/2011jd017074, 2012.
- 1346 Sharma, S., Barrie, L. A., Magnusson, E., Brattstrom, G., Leaitch, W. R., Steffen, A., and Landsberger,
1347 S.: A Factor and Trends Analysis of Multidecadal Lower Tropospheric Observations of Arctic Aerosol
1348 Composition, Black Carbon, Ozone, and Mercury at Alert, Canada, *Journal of Geophysical Research-
1349 Atmospheres*, 124, 14133-14161, 10.1029/2019jd030844, 2019.
- 1350 Shaw, G. E.: The arctic haze phenomenon, *Bulletin of the American Meteorological Society*, 76, 2403-
1351 2413, 10.1175/1520-0477(1995)076<2403:tahp>2.0.co;2, 1995.
- 1352 Simoneit, B. R. T., Schauer, J. J., Nolte, C. G., Oros, D. R., Elias, V. O., Fraser, M. P., Rogge, W. F.,
1353 and Cass, G. R.: Levoglucosan, a tracer for cellulose in biomass burning and atmospheric particles,

- 1354 Atmospheric Environment, 33, 173-182, 10.1016/s1352-2310(98)00145-9, 1999.
- 1355 Simpson, D., Yttri, K. E., Klimont, Z., Kupiainen, K., Caseiro, A., Gelencser, A., Pio, C., Puxbaum, H.,
1356 and Legrand, M.: Modeling carbonaceous aerosol over Europe: Analysis of the CARBOSOL and EMEP
1357 EC/OC campaigns, *Journal of Geophysical Research-Atmospheres*, 112, 10.1029/2006JD008158, 2007.
- 1358 Solomon, A., de Boer, G., Creamean, J. M., McComiskey, A., Shupe, M. D., Maahn, M., and Cox, C.:
1359 The relative impact of cloud condensation nuclei and ice nucleating particle concentrations on phase
1360 partitioning in Arctic mixed-phase stratocumulus clouds, *Atmospheric Chemistry and Physics*, 18,
1361 17047-17059, 10.5194/acp-18-17047-2018, 2018.
- 1362 Stohl, A., Forster, C., Frank, A., Seibert, P., and Wotawa, G.: Technical note: The Lagrangian particle
1363 dispersion model FLEXPART version 6.2, *Atmospheric Chemistry and Physics*, 5, 2461-2474,
1364 10.5194/acp-5-2461-2005, 2005.
- 1365 Stohl, A., Andrews, E., Burkhardt, J. F., Forster, C., Herber, A., Hoch, S. W., Kowal, D., Lunder, C.,
1366 Mefford, T., Ogren, J. A., Sharma, S., Spichtinger, N., Stebel, K., Stone, R., Strom, J., Torseth, K.,
1367 Wehrli, C., and Yttri, K. E.: Pan-Arctic enhancements of light absorbing aerosol concentrations due to
1368 North American boreal forest fires during summer 2004, *Journal of Geophysical Research-*
1369 *Atmospheres*, 111, 10.1029/2006JD007216, 2006.
- 1370 Stohl, A., Berg, T., Burkhardt, J. F., Fjaeraa, A. M., Forster, C., Herber, A., Hov, O., Lunder, C.,
1371 McMillan, W. W., Oltmans, S., Shiobara, M., Simpson, D., Solberg, S., Stebel, K., Strom, J., Torseth,
1372 K., Treffeisen, R., Virkkunen, K., and Yttri, K. E.: Arctic smoke - record high air pollution levels in the
1373 European Arctic due to agricultural fires in Eastern Europe in spring 2006, *Atmospheric Chemistry and*
1374 *Physics*, 7, 511-534, 2007.
- 1375 Stohl, A., Klimont, Z., Eckhardt, S., Kupiainen, K., Shevchenko, V. P., Kopeikin, V. M., and
1376 Novigatsky, A. N.: Black carbon in the Arctic: the underestimated role of gas flaring and residential
1377 combustion emissions, *Atmospheric Chemistry and Physics*, 13, 8833-8855, 10.5194/acp-13-8833-
1378 2013, 2013.
- 1379 Surratt, J. D., Chan, A. W. H., Eddingsaas, N. C., Chan, M. N., Loza, C. L., Kwan, A. J., Hersey, S. P.,
1380 Flagan, R. C., Wennberg, P. O., and Seinfeld, J. H.: Reactive intermediates revealed in secondary
1381 organic aerosol formation from isoprene, *Proceedings of the National Academy of Sciences of the*
1382 *United States of America*, 107, 6640-6645, 10.1073/pnas.091114107, 2010.
- 1383 Tobo, Y., Adachi, K., DeMott, P. J., Hill, T. C. J., Hamilton, D. S., Mahowald, N. M., Nagatsuka, N.,
1384 Ohata, S., Uetake, J., Kondo, Y., and Koike, M.: Glacially sourced dust as a potentially significant
1385 source of ice nucleating particles, *Nature Geoscience*, 12, 253-+, 10.1038/s41561-019-0314-x, 2019.
- 1386 Tobler, A. K., Skiba, A., Canonaco, F., Mocnik, G., Rai, P., Chen, G., Bartyzel, J., Zimnoch, M.,
1387 Styszko, K., Necki, J., Furger, M., Rózanski, K., Baltensperger, U., Slowik, J. G., and Prevot, A. S. H.:
1388 Characterization of non-refractory (NR) PM₁ and source apportionment of organic aerosol in Krakow,
1389 Poland, *Atmospheric Chemistry and Physics*, 21, 14893-14906, 10.5194/acp-21-14893-2021, 2021.
- 1390 Tonon, T., Li, Y., and McQueen-Mason, S.: Mannitol biosynthesis in algae: more widespread and
1391 diverse than previously thought, *New Phytologist*, 213, 1573-1579, 10.1111/nph.14358, 2017.
- 1392 Turpin, B. J., and Lim, H. J.: Species contributions to PM_{2.5} mass concentrations: Revisiting common
1393 assumptions for estimating organic mass, *Aerosol Science and Technology*, 35, 602-610,
1394 10.1080/02786820119445, 2001.

- 1395 van der Werf, G. R., Randerson, J. T., Giglio, L., van Leeuwen, T. T., Chen, Y., Rogers, B. M., Mu, M.
 1396 Q., van Marle, M. J. E., Morton, D. C., Collatz, G. J., Yokelson, R. J., and Kasibhatla, P. S.: Global fire
 1397 emissions estimates during 1997-2016, *Earth System Science Data*, 9, 697-720, 10.5194/essd-9-697-
 1398 2017, 2017.
- 1399 Vegetation in Svalbard: <https://www.npolar.no/en/themes/vegetation-svalbard/>, last access: 9 February
 1400 2023.
- 1401 von Schneidemesser, E., Schauer, J. J., Hagler, G. S. W., and Bergin, M. H.: Concentrations and sources
 1402 of carbonaceous aerosol in the atmosphere of Summit, Greenland, *Atmospheric Environment*, 43, 4155-
 1403 4162, 10.1016/j.atmosenv.2009.05.043, 2009.
- 1404 Waked, A., Favez, O., Alleman, L. Y., Piot, C., Petit, J. E., Delaunay, T., Verlinden, E., Golly, B.,
 1405 Besombes, J. L., Jaffrezo, J. L., and Leoz-Garziandia, E.: Source apportionment of PM₁₀ in a north-
 1406 western Europe regional urban background site (Lens, France) using positive matrix factorization and
 1407 including primary biogenic emissions, *Atmospheric Chemistry and Physics*, 14, 3325-3346,
 1408 10.5194/acp-14-3325-2014, 2014.
- 1409 Wennberg, P. O., Bates, K. H., Crouse, J. D., Dodson, L. G., McVay, R. C., Mertens, L. A., Nguyen,
 1410 T. B., Praske, E., Schwantes, R. H., Smarte, M. D., St Clair, J. M., Teng, A. P., Zhang, X., and Seinfeld,
 1411 J. H.: Gas-Phase Reactions of Isoprene and Its Major Oxidation Products, *Chemical Reviews*, 118, 3337-
 1412 3390, 10.1021/acs.chemrev.7b00439, 2018.
- 1413 Winiger, P., Andersson, A., Yttri, K. E., Tunved, P., and Gustafsson, O.: Isotope-Based Source
 1414 Apportionment of EC Aerosol Particles during Winter High-Pollution Events at the Zeppelin
 1415 Observatory, Svalbard, *Environmental Science & Technology*, 49, 11959-11966,
 1416 10.1021/acs.est.5b02644, 2015.
- 1417 Williams, J. and Koppmann, R.J. (2007) Volatile organic compounds in the atmosphere: An overview.
 1418 In: Volatile organic compounds in the atmosphere. Ed. by: R. Koppmann. Oxford, Blackwell Publishing.
 1419 pp. 1-19.
- 1420 Winiger, P., Barrett, T. E., Sheesley, R. J., Huang, L., Sharma, S., Barrie, L. A., Yttri, K. E., Evangelidou,
 1421 N., Eckhardt, S., Stohl, A., Klimont, Z., Heyes, C., Semiletov, I. P., Dudarev, O. V., Charkin, A.,
 1422 Shakhova, N., Holmstrand, H., Andersson, A., and Gustafsson, O.: Source apportionment of circum-
 1423 Arctic atmospheric black carbon from isotopes and modeling, *Science Advances*, 5,
 1424 10.1126/sciadv.aau8052, 2019.
- 1425 Xia, X., and Hopke, P. K.: Seasonal variation of 2-methyltetrols in ambient air samples, *Environmental
 1426 Science & Technology*, 40, 6934-6937, 10.1021/es060988l, 2006.
- 1427 Yttri, K. E., Aas, W., Bjerke, A., Cape, J. N., Cavalli, F., Ceburnis, D., Dye, C., Emblico, L., Facchini,
 1428 M. C., Forster, C., Hanssen, J. E., Hansson, H. C., Jennings, S. G., Maenhaut, W., Putaud, J. P., and
 1429 Torseth, K.: Elemental and organic carbon in PM₁₀: a one year measurement campaign within the
 1430 European Monitoring and Evaluation Programme EMEP, *Atmospheric Chemistry and Physics*, 7, 5711-
 1431 5725, 2007b.
- 1432 Yttri, K. E., Dye, C., and Kiss, G.: Ambient aerosol concentrations of sugars and sugar-alcohols at four
 1433 different sites in Norway, *Atmospheric Chemistry and Physics*, 7, 4267-4279, 2007a.
- 1434 Yttri, K. E., Simpson, D., Nojgaard, J. K., Kristensen, K., Genberg, J., Stenstrom, K., Swietlicki, E.,
 1435 Hillamo, R., Aurela, M., Bauer, H., Offenberg, J. H., Jaoui, M., Dye, C., Eckhardt, S., Burkhardt, J. F.,
 1436 Stohl, A., and Glasius, M.: Source apportionment of the summer time carbonaceous aerosol at Nordic

- 1437 rural background sites, *Atmospheric Chemistry and Physics*, 11, 13339-13357, 10.5194/acp-11-13339-
1438 2011, 2011b.
- 1439 Yttri, K. E., Simpson, D., Stenstrom, K., Puxbaum, H., and Svendby, T.: Source apportionment of the
1440 carbonaceous aerosol in Norway - quantitative estimates based on C-14, thermal-optical and organic
1441 tracer analysis, *Atmospheric Chemistry and Physics*, 11, 9375-9394, 10.5194/acp-11-9375-2011, 2011a.
- 1442 Yttri, K. E., Myhre, C. L., Eckhardt, S., Fiebig, M., Dye, C., Hirdman, D., Stroem, J., Klimont, Z., and
1443 Stohl, A.: Quantifying black carbon from biomass burning by means of levoglucosan - a one-year time
1444 series at the Arctic observatory Zeppelin, *Atmospheric Chemistry and Physics*, 14, 6427-6442,
1445 10.5194/acp-14-6427-2014, 2014.
- 1446 Yttri, K. E., Canonaco, F., Eckhardt, S., Evangeliou, N., Fiebig, M., Gundersen, H., Hjellbrekke, A. G.,
1447 Myhre, C. L., Platt, S. M., Prevot, A. S. H., Simpson, D., Solberg, S., Surratt, J., Torseth, K., Uggerud,
1448 H., Vadset, M., Wan, X., and Aas, W.: Trends, composition, and sources of carbonaceous aerosol at the
1449 Birkenes Observatory, northern Europe, 2001-2018, *Atmospheric Chemistry and Physics*, 21, 7149-
1450 7170, 10.5194/acp-21-7149-2021, 2021.
- 1451 Zangrando, R., Barbaro, E., Zennaro, P., Rossi, S., Kehrwald, N. M., Gabrieli, J., Barbante, C., and
1452 Gambaro, A.: Molecular Markers of Biomass Burning in Arctic Aerosols, *Environmental Science &
1453 Technology*, 47, 8565-8574, 10.1021/es400125r, 2013.
- 1454 Zieger, P., Heslin-Rees, D., Karlsson, L., Koike, M., Modini, R., and Krejci, R.: Black carbon
1455 scavenging by low-level Arctic clouds, *Nature Communications*, 14, 10.1038/s41467-023-41221-w,
1456 2023.
- 1457 Zwaafink, C. D. G., Grythe, H., Skov, H., and Stohl, A.: Substantial contribution of northern high-
1458 latitude sources to mineral dust in the Arctic, *Journal of Geophysical Research-Atmospheres*, 121,
1459 13678-13697, 10.1002/2016jd025482, 2016.
- 1460 Zwaafink, C. D. G., Aas, W., Eckhardt, S., Evangeliou, N., Hamer, P., Johnsrud, M., Kylling, A., Platt,
1461 S. M., Stebel, K., Uggerud, H., and Yttri, K. E.: What caused a record high PM10 episode in northern
1462 Europe in October 2020?, *Atmospheric Chemistry and Physics*, 22, 3789-3810, 10.5194/acp-22-3789-
1463 2022, 2022.

Table 1: Annual and seasonal mean concentrations of OC, OC_B (OC on backup filters) EC, TC, and organic tracers at Zeppelin Observatory, 2017 to 2020.

	OC (ng C m ⁻³)	OC _B (ng C m ⁻³)	EC (ng C m ⁻³)	TC (ng C m ⁻³)	Cellul. (ng m ⁻³)	Levo-gl. (pg m ⁻³)	Mannos. (pg m ⁻³)	Galactos. (pg m ⁻³)	Arabitol (pg m ⁻³)	Mannitol (pg m ⁻³)	Fructose (pg m ⁻³)	Glucose (pg m ⁻³)	Trehalose (pg m ⁻³)	2-methylery. (pg m ⁻³)	2-methylthir. (pg m ⁻³)
2017	121	32.9	11.6	132	2.1	465	53.5	18.7	99.7	115	80.9	250	140	99.2	43.7
DJF	99.6		14.8	116	2.1	862	120	38.1	29.5	29.7	130	106	31.7	5.6	3.5
MAM	128		20.8	149	2.1	83.4	11.9	3.5	7.7	15.1	32.4	123	64.0	6.1	3.8
JJA	94.5		3.5	97.6	1.6	160	33.2	10.8	70.2	93.1	58.6	189	154	205	87.6
SON	146		9.7	156	2.4	725	59.4	23.8	235	260	1051	484	251	134	59.7
2018	90.3	22.0	6.5	96.1	1.2	335	62.7	22.4	59.1	69.4	63.9	269	71.8	80.9	43.1
DJF	88.5		9.7	98.1	1.3	587	66.3	22.6	38.6	49.7	105	137	37.6	4.8	2.8
MAM	101		11.3	112	1.3	150	15.0	8.0	11.8	15.3	55.5	183	43.9	13.2	8.4
JJA	123		4.5	127	1.4	481	113	42.4	137	156	84.1	494	144	217	113
SON	48.3		3.0	50.3	0.9	236	52.7	14.8	31.7	38.9	32.2	176	39.2	38.4	21.8
2019	102	24.2	12.5	115	1.3	547	120	30.2	138	161	90.7	504	217	251	113
DJF	109		24.2	133	1.3	1124	152	38.6	27.0	18.4	62.0	583	47.4	7.1	5.5
MAM	79.0		15.1	94.1	1.2	127	19.8	5.6	10.7	17.0	49.2	209	135	6.5	4.0
JJA	169		9.2	178	1.6	530	181	47.8	265	306	107	707	250	812	366
SON	63.1		3.6	66.5	1.0	565	148	34.8	251	301	144	581	410	212	93.1
2020	197	32.6	16.3	214	1.6	919	175	54.7	242	172	179	808	188	644	502
DJF	85.9		14.5	101	1.5	1370	205	69.6	29.0	25.6	75.7	431	64.6	7.4	4.5
MAM	137		25.2	163	1.2	229	29.3	12.3	22.5	22.7	24.3	145	36.3	15.5	8.8
JJA	334		10.8	345	1.9	1292	299	86.2	659	415	473	2160	386	2350	1850
SON	202		13.7	216	2.1	963	188	58.8	226	207	129	424	260	47.5	24.0
Mean ±SD															
Annual	128±48.0	27.9±5.6	11.7±4.0	139±51.7	1.6±0.2	567±251	103±56.2	31.5±16.2	135±78.5	129±46.8	104±51.5	457±260	154±63.6	267±261	176±220
DJF	95.8±11.0		15.8±6.1	112±16.2	1.5±0.4	986±337	136±58.0	42.2±19.7	31.0±5.2	30.9±13.4	93.0±30.2	314±213	45.3±14.4	6.2±1.2	4.1±1.2
MAM	111±26.1		18.1±6.1	129±31.8	1.4±0.4	147±61.0	19.0±7.6	7.4±3.8	13.2±6.5	17.±3.6.	40.4±14.5	168±38.5	69.9±45.1	10.3±4.7	6.3±2.7
JJA	180±107		7.0±3.5	187±110	1.6±0.1	616±480	157±113	46.8±30.9	283±264	243±146	181±196	888±876	234±113	896±1010	604±839
SON	115±72.3		7.5±5.1	122±77.8	1.6±0.7	622±305	112±66.6	33.1±19.0	186±103	202±115	103±49.4	416±173	240±152	108±81.4	49.7±33.8
H-S	102±19.0		15.7±4.1	117±23.0	1.5±0.4	518±156	68.9±24.7	22.8±9.4	23.7±3.6	26.1±2.0	77.3±21.8	233±105	79±63	9.2±3.0	5.7±1.7
NH-S	152±75.0		7.6±3.3	163±86.0	1.7±0.5	622±374	152±111	41.4±25.3	258±160	246±108	148±115	703±472	235±96	555±530	360±445

Notations: H-S = Heating season (November to May); NH-S = Non-heating season (June - October)

Table 2: Estimated annual mean concentrations (eq. 1 – 7) of sea salt aerosol (SSA), mineral dust (MD), non-sea salt sulfate (nss-SO₄²⁻), organic matter (OM = OC × 2.2; Turpin and Lim, 2001), and elemental carbon (EC) at Zeppelin Observatory 2017 to 2020. Unit: ng m⁻³.

	SSA	MD¹⁾	nss-SO₄²⁻	OM	EC
2017	730	559	381	265	11.6
2018	618	279	243	199	6.5
2019	697	477	283	225	12.5
2020	684	1136	349	434	16.3
Mean ± SD	682 ± 46.9	613 ± 368	314 ± 62.6	281 ± 106	12 ± 4.0

1) 3 μm EAD size fraction (10 μm EAD for other variables).

Table 3: Annual, heating season, and non-heating season contributions of BB and FF to eBC (PMF) and BC (FLEXPART). BB is denoted RWC in the heating season and WF in the non-heating season. Heating season and non-heating season contributions of levoglucosan are included. Zeppelin Observatory, 2017 to 2020. Unit: %.

	2017			2018			2019			2020			Mean \pm SD	
	PMF	FLEXPART		PMF	FLEXPART		PMF	FLEXPART		PMF	FLEXPART		PMF	FLEXPART
Annual														
eBC_{FF}/eBC	71	54	68	47	53	67	50	50	50	70	2.7	51	3.1	
eBC_{BB}/eBC	29	46	32	53	47	33	50	50	50	30	2.7	49	3.1	
Heating season														
eBC_{FF}/eBC	73	59	67	51	58	70	57	57	57	71	2.7	56	3.6	
eBC_{RWC}/eBC	27	41	33	49	42	30	43	43	43	29	2.7	44	3.6	
Non-heating season														
eBC_{FF}/eBC	65	43	72	35	41	58	37	37	37	67	6.7	39	3.3	
eBC_{WF}/eBC	35	57	28	65	59	42	63	63	63	33	6.7	61	3.3	
Seasonal/Annual														
eBC_{FF_H-S}/eBC_{FF}	77	73	80	80	79	75	74	74	74	77	1.8	77	3.8	
eBC_{FF_NH-S}/eBC_{FF}	23	27	20	20	21	25	26	26	26	23	1.8	23	3.8	
eBC_{RWC}/eBC_{BB}	69	58	83	68	65	65	55	55	55	74	8.2	62	6.0	
eBC_{WF}/eBC_{BB}	31	42	17	32	35	35	45	45	45	26	8.2	38	6.0	
Seasonal/Annual														
eBC_{FF_H-S}/eBC	55	39	54	38	42	50	37	37	37	54	2.8	39	2.4	
eBC_{FF_NH-S}/eBC	16	14	14	9	11	17	13	13	13	16	1.2	12	2.3	
eBC_{RWC}/eBC	20	27	26	36	31	22	28	28	28	22	2.7	30	4.1	
eBC_{WF}/eBC	8.9	20	5.4	17	16	12	22	22	22	8.0	2.9	19	2.8	

Notation: eBC = equivalent black carbon; FF = fossil fuel; BB = biomass burning; H-S = Heating season; NH-S = Non-heating season; WF = Wildfire; RWC = Residential wood combustion; For simplicity we state eBC for both PMF and FLEXPART methods, while the correct is BC for FLEXPART.

Table 4: BB and FF fractions of BC (monthly weighted) obtained by different approaches (PMF, FLEXPART, and Radiocarbon;LHS) for non-heating-season and heating season. Means are based on identical time periods (See Table S3).

Methodology	Annual		NH-season (JJASO)		H-season (NDJFMAM)	
	BC _{BB} /BC	BC _{FF} /BC	BC _{BB} /BC	BC _{FF} /BC	BC _{BB} /BC	BC _{FF} /BC
PMF	27 ± 14	73 ± 14	31 ± 11	69 ± 11	25 ± 16	75 ± 16
FLEXPART	45 ± 5	55 ± 5	48 ± 18	52 ± 18	42 ± 10	58 ± 10
Radiocarbon;LHS	61 ± 15	39 ± 15	67 ± 5	33 ± 5	57 ± 18	43 ± 18

Notation: For simplicity we state BC for all methods, while the correct is eBC for PMF, BC for FLEXPART, and EC for Radiocarbon;LHS.



Figure 1. The Zeppelin observatory located at the Zeppelin Mountain (472 m a.s.l.) close to the Ny-Ålesund settlement at Svalbard ($78^{\circ}54'0''\text{ N}$, $11^{\circ}53'0''\text{ E}$) in: winter (left panel); summer (middle panel); The light-blue line on the map shows the Arctic Circle (66° North) (right panel). (Foto: Ove Hermansen, NILU; Map: Finn Bjørklid, NILU).

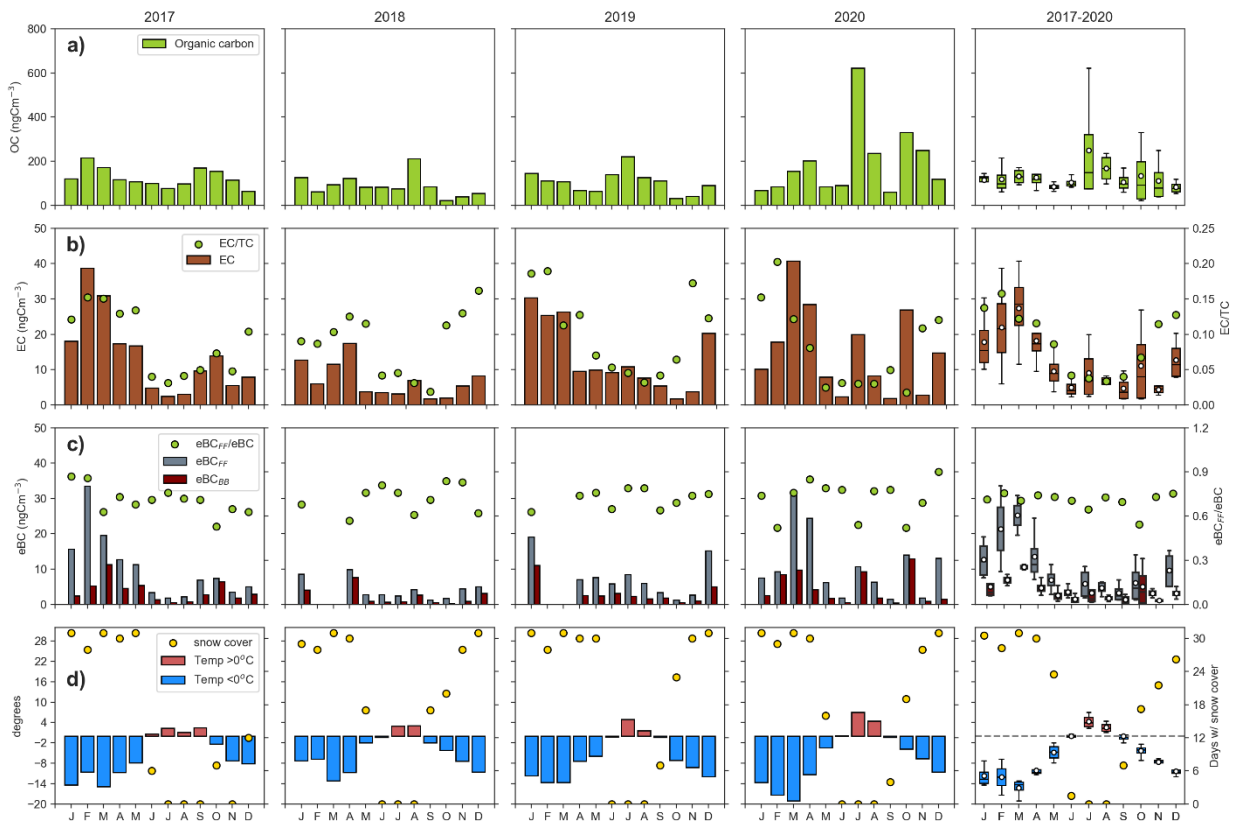


Figure 2. Panels show monthly mean concentrations for 2017 to 2020 and box plots (mean, 25, 50, 75 percentiles and IQR) for 2017 to 2020 at Zeppelin Observatory for a) OC; b) EC and EC/TC; c) eBC_{BB}, eBC_{FF}, and eBC_{FF}/eBC; d) Ambient temperature and days with snow on ground. Concentrations in a) - c) are measured in the PM₁₀ size fraction.

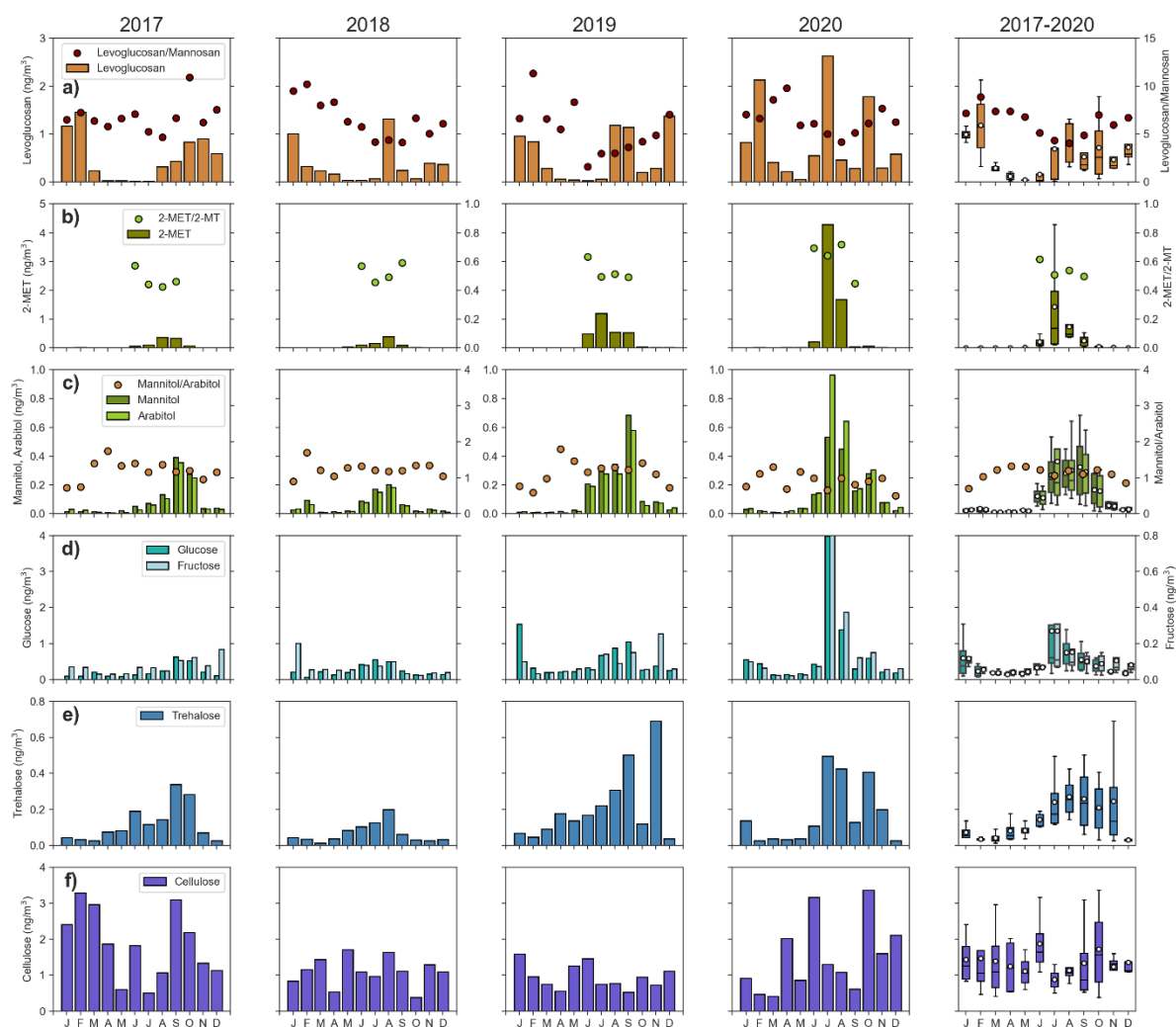


Figure 3. Panels show monthly mean concentrations for 2017 to 2020 and box plots (mean, 25, 50, 75 percentiles and IQR) for 2017 to 2020 at Zeppelin Observatory for a) Levoglucosan and levoglucosan/mannosan; b) 2-methylerythritol (2-MET) and 2-MT/2-MET; c) Mannitol and arabitol and mannitol/arabitol; d) Fructose and glucose; e) Trehalose; f) Cellulose. All variables are measured in the PM_{10} size fraction.

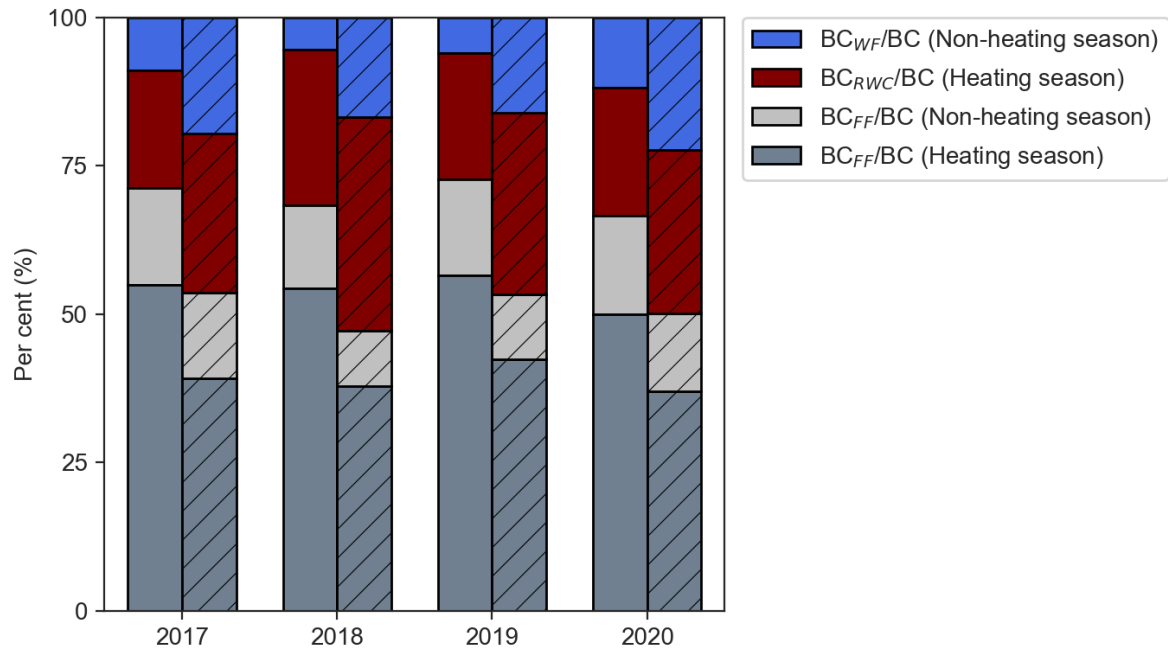


Figure 4. eBC (PMF) (without diagonal lines) and BC (FLEXPART) (with diagonal lines) apportioned to biomass burning (BB) and fossil (FF) fuel combustion according to heating season and non-heating season. BB is denoted wildfire (WF) in summer and residential wood combustion (RWC) in winter. Zeppelin Observatory (2017 to 2020). For simplicity we state BC for all methods, while the correct is eBC for PMF, BC for FLEXPART.

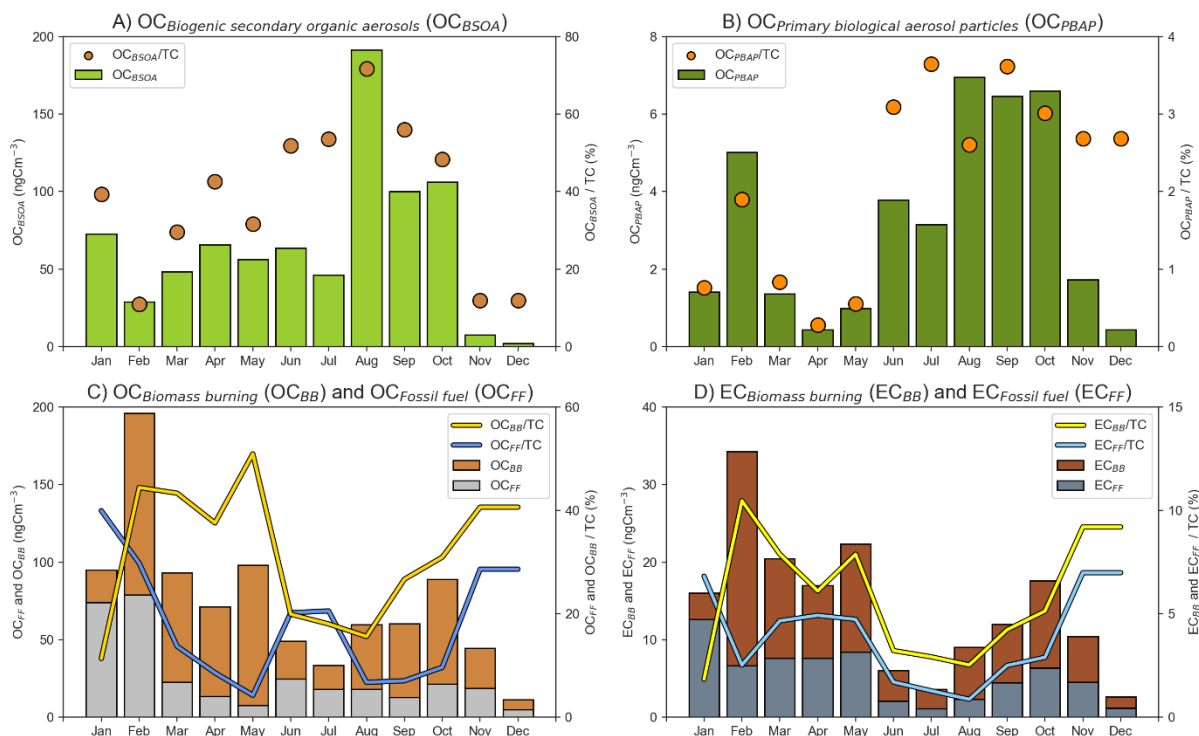


Figure 5. Source apportionment using the LHS approach (Sect. 2.7). Panels show monthly mean concentrations and relative contributions for samples collected in 2017 to 2018 at Zeppelin Observatory for A) Biogenic Secondary Organic Aerosol (OC_{BSOA}) and OC_{BSOA}/TC; B) Primary Biological Aerosol Particles (OC_{PBAP}), being the sum of fungal spores (OC_{PBS}) and plant debris (OC_{PBC}), and OC_{PBAP}/TC; C) Biomass burning (OC_{BB}, OC_{BB}/TC) and fossil fuel sources (OC_{FF}, OC_{FF}/TC; D) Fossil fuel (EC_{FF}, EC_{FF}/TC) and biomass burning (EC_{BB}, EC_{BB}/TC).

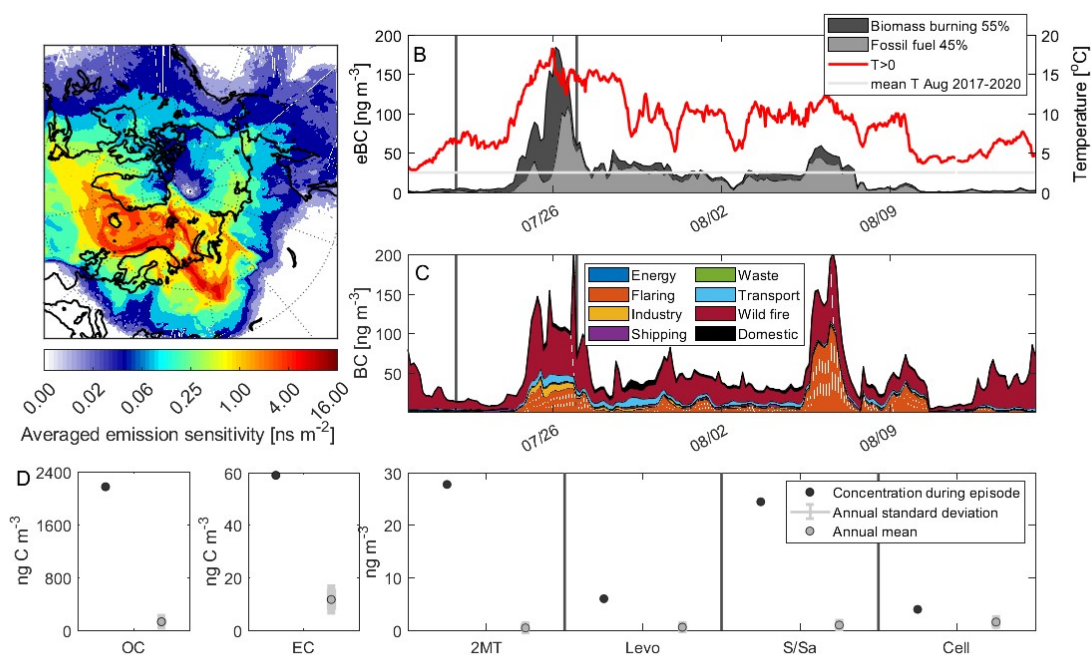


Figure 6. LRT episode at Zeppelin Observatory covered by filter sample collected 22 – 27.07.2020. A) Averaged footprint sensitivity for sample collected 22 – 27.07.2020; B) Hourly time series of eBC_{BB} and eBC_{FF} (PMF) and ambient temperature. The period covered by the filter sample is defined by the dark grey vertical lines; C) Hourly time series of modelled BC concentrations from different source categories; D) Concentrations of OC, EC, and organic tracers (2MT = 2-Methyltetrols; Levo = Levoglucosan; S and SA = Sugars and Sugar-alcohols; Cell = Cellulose) obtained for the filter sample compared to the long-term annual mean and its standard deviation.

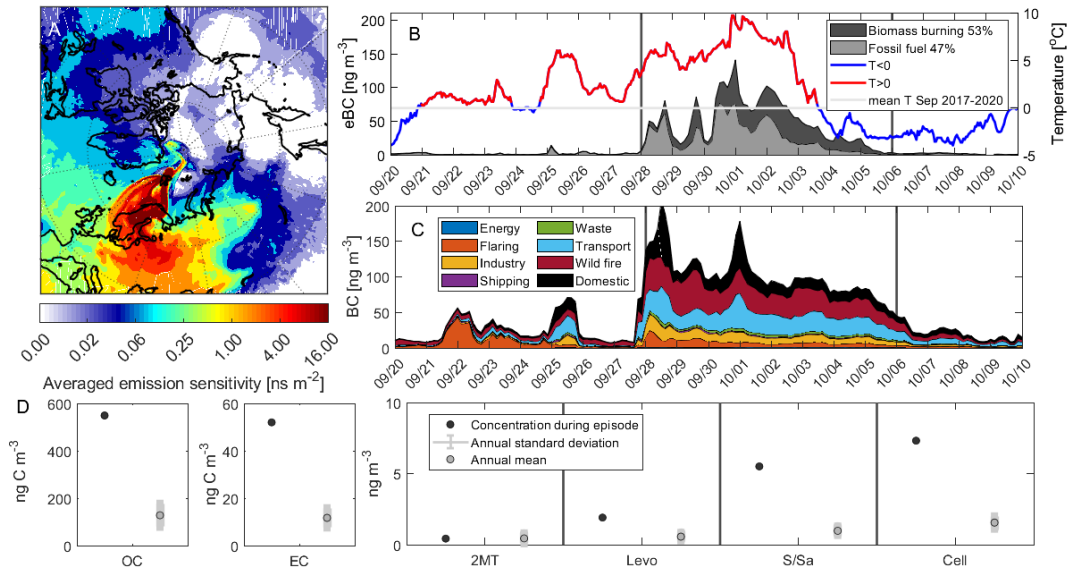


Figure 7. Same as Fig. 6, but for 28.09 – 06.10.2017.

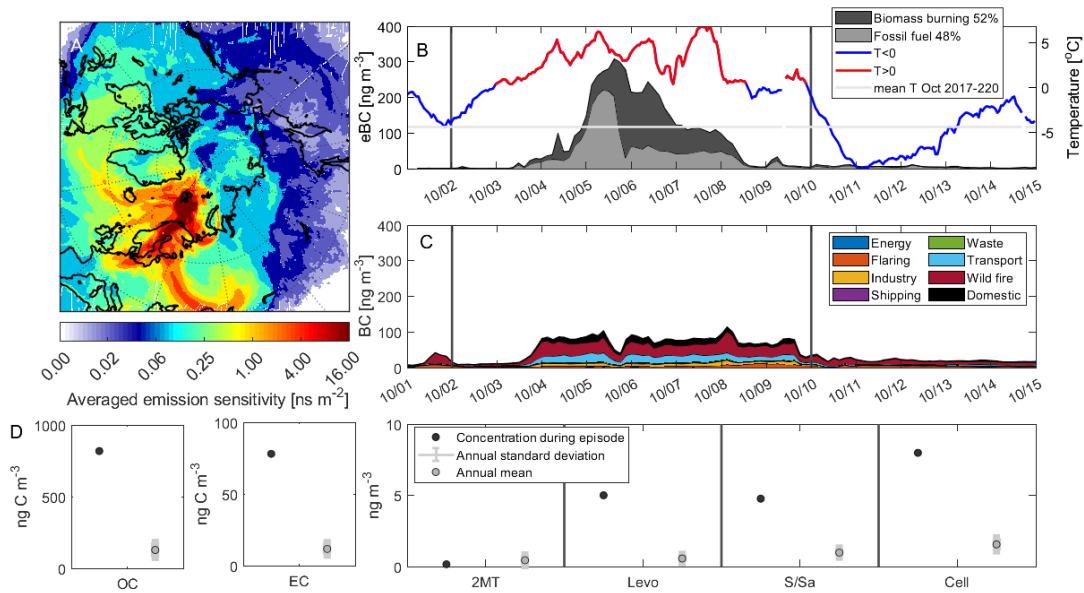


Figure 8. Same as Fig. 6, but for 2 – 10.10.2020.